

# Developing a Test Method to Investigate Water Susceptibility of Joint and Crack Sealants

FINAL PROJECT REPORT

by

## Principal Investigator:

Elham (Ellie) H. Fini, Ph.D., P.E. ([efini@ncat.edu](mailto:efini@ncat.edu))

Ahmed Lamarre: [aplamar@aggies.ncat.edu](mailto:aplamar@aggies.ncat.edu)

Shahrzad Hossein Nezhad: [shossein@aggies.ncat.edu](mailto:shossein@aggies.ncat.edu)

Sponsorship

Center for Highway Pavement Preservation(CHPP) &  
North Carolina A&T State University

for

Center for Highway Pavement Preservation  
(CHPP)



In cooperation with US Department of Transportation-Research and Innovative Technology  
Administration (RITA)

October 31, 2016

## **DISCLAIMER**

The contents of this report reflect the views of the authors, who are responsible for the facts and the accuracy of the information presented herein. This document is disseminated under the sponsorship of the U.S. Department of Transportation's University Transportation Centers Program, in the interest of information exchange. The Center for Highway Pavement Preservation (CHPP), the U.S. Government and matching sponsor assume no liability for the contents or use thereof.

## **ACKNOWLEDGEMENT**

The authors would like to acknowledge the support provided by the USDOT through the University Transportation Center: Center for Highway Pavement Preservation led by Michigan State University. The contents of this report is based on the results of experiments and analysis performed under this project and reflect the view of the authors, who are responsible for the facts and the accuracy of the data presented. We would like to thank NC A&T's Sustainable Infrastructure Materials (SIM) Lab's personnel and students who assisted the research team with the conduct of the experiments. We are also thankful for the support of the CHPP Advisory committee who provided great comments, suggestions and constructive feedback on our research plan and methodology both at the proposal stage and during the project tenure when presented our midterm results at the meeting in East Lansing, MI (February 19, 2016). We also appreciate assistance from Dr. Imad Al-Qadi and Dr. Hassan Ozer with the University of Illinois Urbana-Champaign for providing the laboratory and field aged sealant samples for the study and for their very valuable inputs during the project. We specially appreciate the center administration for their leadership and assistance with productive and efficient operation of this partnership and center activities. Their effort in making sure all findings are well disseminated via CHPP center's websites, conferences, workshops and publication played a strong role in the success of the center. In addition, their meticulous compilation and review of the projects' progress report as well as holding meetings, organizing outreach programs and retreats were crucial for the success of the center.

Technical Report Documentation Page			
1. Report No.	2. Government Accession No.	3. Recipient's Catalog No.	
4. Title and Subtitle Developing a Test Method to Investigate Water Susceptibility of Joint and Crack Sealants		5. Report Date: Oct. 31, 2016	
		6. Performing Organization Code	
7. Author(s) Elham (Ellie) H. Fini, Ph.D., P.E. (efini@ncat.edu) Ahmed Lamarre: aplamarr@aggies.ncat.edu Shahrzad Hossein Nezhad: shossein@aggies.ncat.edu		8. Performing Organization Report No.	
9. Performing Organization Name and Address: North Carolina A&T State University CHPP Center for Highway Pavement Preservation, Tier 1 University Transportation Center Michigan State University, 2857 Jolly Road, Okemos, MI 48864		10. Work Unit No. (TRAIS)	
		11. Contract or Grant No.	
12. Sponsoring Organization Name and Address  United States of America Department of Transportation Research and Innovative Technology Administration		13. Type of Report and Period Covered UTC:CHPP-Cycle 1 & 2	
		14. Sponsoring Agency Code	
15. Supplementary Notes Report uploaded at <a href="http://www.chpp.egr.msu.edu/">http://www.chpp.egr.msu.edu/</a>			
16. Abstract Sealants are commonly used to insulate cracks and joints preventing water from entering the underlying structure. However, extended exposure of sealants to water has shown to negatively impact sealants properties causing gradual degradation of sealant performance. While there have been many studies on characterizing sealant performance in dry conditions, there has been no comprehensive experimental tests to evaluate crack sealants water susceptibility based on a fundamental material property. This study introduces five laboratory tests to investigate the effect of water exposure on different crack sealants commonly used in cold, moderate and hot climates. Sealants were acquired in collaboration with University of Illinois Urbana-Champaign. Experimental plan includes several thermo-mechanical and surface characterization tests. Crack sealants' rheological properties and relaxation time was measured using a Dynamic Shear Rheometer (DSR). Sealants' creep compliance was measured using an extended Bending Beam Rheometer (BBR). In addition, a direct adhesion test was incorporated using a Direct Adhesion Test (DAT) machine to determine the load required to bring sealant specimen to adhesion failure. Surface tension was measured using a Goniometer. A higher reduction in surface tension indicates sealant has more susceptibility to water. Chemical structure and formation of any new functional groups was tracked using Fourier Transform Infrared (FTIR) spectroscopy. The extent of change in aforementioned sealant properties before and after water conditioning was used as indicators of sealant susceptibility to water. The experiments results were compared against sealants' field performance data obtained through the Pooled-Fund Crack Sealant Consortium led by the University of Illinois at Urbana Champaign.			
17. Key Words: sealant, rheology, surface morphology, moisture, water susceptibility, adhesion, cohesion		18. Distribution Statement  No restrictions.	
19. Security Classification (of this report) Unclassified.	20. Security Classification (of this page) Unclassified.	21. No. of Pages: 64	22. Price NA

## **Executive Summary:**

Sealants are commonly used to insulate cracks and joints preventing water from entering the underlying structure. However, extended exposure of sealants to water has shown to negatively impact sealants properties causing gradual degradation of sealant performance. In addition, sealants show different degradation rates when they are exposed to water depending on their chemical composition and environmental conditions. While there have been many studies on characterizing sealant performance in dry conditions, there has been no comprehensive experimental tests to evaluate crack sealants water susceptibility based on a fundamental material property. This study introduces five laboratory tests to investigate the effect of water exposure on different crack sealants commonly used in cold, moderate and hot climates. The first test examines crack sealants' rheological properties and relaxation time using a Dynamic Shear Rheometer (DSR). The relaxation time, which is the time it takes for the stress to disappear when a constant strain is applied on the crack sealant, is calculated to determine how fast the recovery is happening before and after conditioning.

It is hypothesized that it will take longer for the stress to disappear after the sealant is exposed to water. The second test uses the Bending Beam Rheometer (BBR) machine to measure the crack sealant's ability to resist low temperature cracking. The third test implements a direct adhesion test using a Direct Adhesion Test (DAT) machine to determine the surface energy and load required to cause the sealant's adhesion failure before and after water exposure. The fourth test examines Surface Tension using a Goniometer. A higher reduction in surface tension means more susceptibility to water exposure. The fifth and final test identifies the chemical bonding and functional groups formed before and after water exposure in selected crack sealants using the Fourier Transform Infrared (FTIR). The FTIR spectra can be used to track phenomenon such as oxidation and hydrolysis after water conditioning as a means of sealant water susceptibility. In this study, six different hot-poured crack sealants were investigated using aforementioned methods, and ranked according to the extent of change in their properties. Specifically, the change in sealant's mechanical properties after water exposure was done based on the DSR, BBR and DAT specifications. A new measure (recovery) was also developed based on the extended BBR test (in which the recovery data was collected for 460s, after the load was removed. The recovered deformation at the mid-span of the beam at 700s (240s loading and 460s after unloading) was used to calculate the recovery (the percentage of recovered deformation at selected temperature). The difference in the recovery ratio among water conditioned and dry samples was used as a measure of sealant susceptibility to water. The experiments results were compared against sealants' field performance data obtained through the Pooled-Fund Crack Sealant Consortium led by the University of Illinois at Urbana Champaign.

To further explain the differential effects of water on various sealants, a preliminary study of wax composition on selected bituminous materials was performed. The study was performed by doping the selected bituminous material with (1-10%) paraffin wax. The analysis results from various mechanical tests reduced affinity for water as the wax percentage was increased. While the wax lamella formed in the bitumen can repel water, they can negatively affect sealant cohesion properties at low temperature. In fact, introduction of wax lead to a significant drop in fracture energy at 1% wax which can be attributed to dominant effect of paraffin wax crystals promoting stress concentration at the wax-bitumen interface. Further study is recommended to provide a more in-depth understanding of property-composition in sealants to develop performance indicators, which are based on fundamental sealant properties. This in turn can help road authorities with their sealant selection and screening while providing manufacturer with more informed strategies for formulating sealants with enhance performance.

## Table of Contents

List of Figures .....	vii
List of Tables .....	ix
Chapter 1 Introduction .....	1
1.1 Background Information.....	1
1.2 Problem Statement .....	2
1.3 Objectives .....	2
1.4 Organization.....	3
Chapter 2 Literature Review of Crack Sealant and Asphalt .....	4
2.1 How to Select Crack Sealant and Asphalt .....	4
2.2 Performance of Crack Sealant and Asphalt .....	5
2.3 Test Methods for Crack Sealant and Asphalt .....	7
2.3.1 Adhesion test.....	7
2.3.2 Sessile drop test.....	9
2.3.3 Dynamic shear rheometer test.....	10
2.3.4 Atomic force microscopy test .....	10
Chapter 3 Methodology .....	12
3.1 Materials .....	12
3.2 Test Methods for Crack Sealant.....	12
3.3 Sessile Drop Methods and Contact Angle .....	13
3.4 Asphalt Test Methods .....	15
Chapter 4 Results .....	19
4.1 Dynamic Shear Rheometer Test .....	19

4.1.1 Crack Sealant .....	19
4.1.2 Asphalt .....	20
4.2 Relaxation and Modulus of Elasticity.....	22
4.2.1 Relaxation .....	22
4.2.2 Modulus of Elasticity.....	25
4.3 Bending Beam Rheometer Test .....	27
4.3.1 Crack Sealant .....	27
4.3.2 Asphalt .....	30
4.4 Direct Adhesion Test .....	31
4.4.1 Crack Sealant .....	31
4.4.2 Asphalt .....	34
4.5 Fourier Transform Infrared Spectroscopy Analysis .....	35
4.6 Sessile Drop Test .....	39
4.7 Crack Sealant Performance.....	41
4.8 Asphalt Performance.....	42
4.8.1 Temperature susceptibility.....	44
4.8.2 Shear susceptibility .....	45
4.9 Direct Tension Test.....	46
4.10 Differential Scanning Calorimetry.....	48
4.11 Atomic Force Microscopy .....	49
Chapter 5 Conclusions .....	51
5.1 Crack Sealant .....	51
5.2 Asphalt .....	52

## List of Figures

Figure 1. Experiment Plan .....	3
Figure 2. (a) FTA-1000 and (b) image of a droplet of water on sealant surface .....	15
Figure 3. Direct Adhesion Test Fixture .....	18
Figure 4. Relaxation Time for Different Aging Methods .....	20
Figure 5a. Rotational Viscometer Results for 0%, 1%, 3%, and 10% Wax-Modified Binder .....	21
Figure 5b. Crossover Temperatures for 0%, 1%, 3%, and 10% Wax-Modified Binder .....	22
Figure 6a. Sealant Relaxation Time Before and After 2 Weeks of Water Exposure.....	23
Figure 6b. Sealant Relaxation Time Before and After Water Exposure.....	24
Figure 6c. Lab-Aged Sealant Relaxation Time Before and After Water Exposure.....	24
Figure 6d. Field-Aged Sealant Relaxation Time Before and After Water Exposure .....	24
Figure 7. Sealants DD, EE, FF, AA, CC, and BB Before and After Water Exposure .....	26
Figure 8a. Bending Beam Rheometer Illustration .....	28
Figure 8b. Bending Beam Rheometer Test Before and After Water Exposure .....	29
Figure 8c. Crack Sealant Recovery Before and After Water Exposure.....	29
Figure 8d. Crack Sealant Recovery Before and After Extended Water Exposure .....	30
Figure 8e. Crack Sealant 50% Slope Before and After Water Exposure.....	30
Figure 9. Stiffness and M-Value Results for 0%, 3%, 5%, and 10% Wax-Modified Binder.....	31
Figure 10a. Fracture Energy Before and After 24 hours of Water Exposure .....	33

Figure 10b. Peak Load Before and After 24 hrs Water Exposure .....	34
Figure 11a. DAT Fracture Energy Results for 0%, 1%, 3%, and 5% Wax-Modified Binder .....	35
Figure 11b. DAT Peak Load Results for 0%, 1%, 3%, and 5% Wax-Modified Binder.....	35
Figure 12a,b,c. Fourier Transform Infrared Spectroscopy Before and After Water Exposure ....	37
Figure 12d. Virgin Fourier Transform Infrared Spectroscopy Before and After Water Exposure.....	38
Figure 12e. Lab-Aged FTIR Before and After Water Exposure .....	38
Figure 12f. Field-Aged FTIR before and after Water Exposure.....	39
Figure 13a. Contact Angle Between Water and Dry Sealant at Various Surface Temperatures ..	40
Figure 13b. Contact Angle Between Water and Water-Conditioned Sealant at Various Surface Temperatures.....	41
Figure 14a. Viscosity vs Temperature at 0%, 1%, 3%, and 5% wax under 50 rpm. ....	43
Figure 14b. Effect of Rotational Speed on Asphalt Binder at 0%, 1%, 3%, and 5% Wax Under 20 rpm and 50 rpm.....	44
Figure 15. Viscosity vs. Temperature for 0%, 1%, 3%, and 5% Wax at 20 rpm .....	45
Figure 16. Shear Susceptibility of 0%, 1%, 3%, and 5% Wax at 20 rpm.....	46
Figure 17a. DTT Fracture Energy for 0%, 1%, 3%, and 5% Wax-Modified Binder .....	47
Figure 17b. DTT Peak Load and Ductility for 0%, 1%, 3%, and 5% Wax-Modified Binder .....	47



Figure 18a. Glass Transition Temperature ( $T_g$ ) for Different Wax-Modified Bitumen, Using the MDSC method .....	48
Figure 18b. Comparison of Heat Capacity of Samples With Different Amounts of Added Wax .....	49
Figure 19a. AFM Images of the Surface of Bitumen Samples Doped With Paraffin Wax (0%, 1%, and 3%, by Weight of Base Asphalt).....	50
Figure 19b. AFM Amplitude Image of the Surface of 10% Wax-Doped Bitumen.....	50

## List of Tables

Table 1. Crack Sealants and Properties.....	15
Table 2. Direct Adhesion Load Test Results Before and After Water Exposure .....	33
Table 3. Direct Adhesion Energy Test Results Before and After Water Exposure .....	33
Table 4. Overall Sealant Performance Based on Water Exposure Test.....	42

## **Chapter 1**

### **Introduction**

#### **1.1 Background Information**

Joints and crack sealants are widely used to protect pavement from the infiltration of water. While typical crack sealants life is between 3-5 years, some studies have shown that joint sealant failure occurs at a rate of 50% in less than 20 years and 95% within 20 years after installation (White et al., 2011). Accordingly, Al-Qadi and his group mdeveloped a series of performance-based tests to characterize sealant bulk and interface properties under dry conditions. They modified existing Superpave testing equipment, including a Rotational Viscometer, a Bending Beam Rheometer, and a Direct Tension Tester, to be used for crack sealant evaluation (Al-Qadi et al., 2009). While the aforementioned tests are comprehensive and accompanied by field validations, they do not address sealant water susceptibility as it relates to sealant surface properties and interface damage. Considering that water plays a major role in deteriorating sealant surface properties and interfacial bonds, there is a need for a fundamental test that can evaluate sealant susceptibility to water.

Sealants are commonly used to insulate cracks and joints, preventing water from entering the underlying structure. However, extended exposure of sealants to water has been shown to negatively impact sealants' properties, causing gradual degradation of sealant performance. In addition, sealants show different degradation rates when they are exposed to water, depending on their chemical composition and environmental conditions. While there have been many studies on characterizing sealant performance in dry conditions, there have been no comprehensive laboratory tests to evaluate crack sealants' water susceptibility based on a fundamental material property.

Edwards and Redelius (2003) studied the rheological effects of adding two bitumen waxes: non-waxy and waxy. The results showed that the magnitude and type of effect on bitumen rheology depends on the bitumen and the type of crystallizing fraction on the bitumen. The DMA used for the study showed stiffening below 50°C for waxy bitumen but not for non-waxy bitumen. It has been reported that the presence of slack wax in bitumen negatively affects the bitumen by lowering the complex modulus at temperatures over 40°C (Fang et al., 2003).

## **1.2 Problem Statement**

- Water exposure causes crack sealant failure.
- Asphalt water exposure affects “bees”, causing adhesion failure.

## **1.3 Objectives**

- Determine the effects of extended water exposure on the rheological properties of crack sealant.
- Evaluate the morphological and rheological properties of sealant exposed to water, and compare them to the properties of virgin sealant.
- Determine the effects of 3%, 5%, and 10% added wax on the rheological properties of asphalt binders.
- Evaluate the physiochemical, morphological, and rheological properties of wax-modified asphalt (WXMA), and compare them to the properties of unmodified asphalt.

### 1.4 Organization

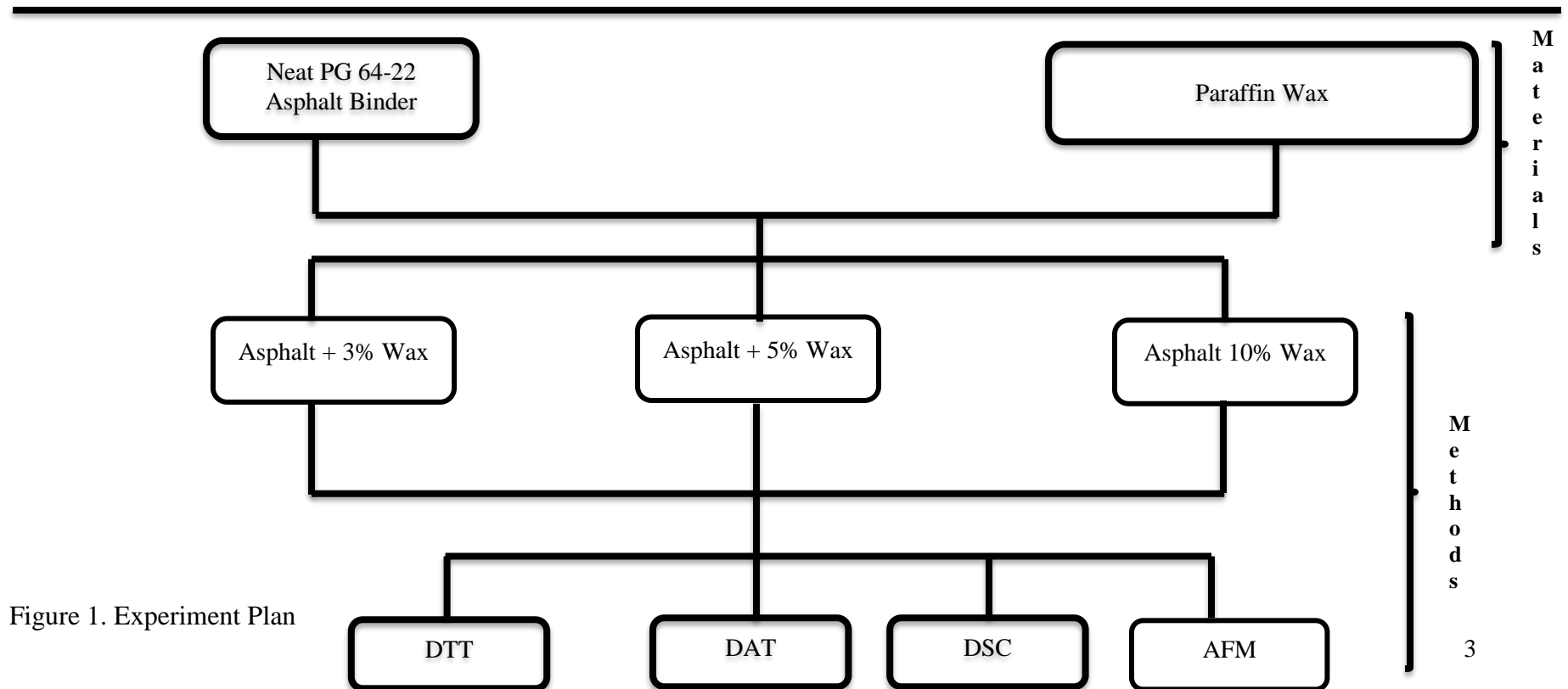
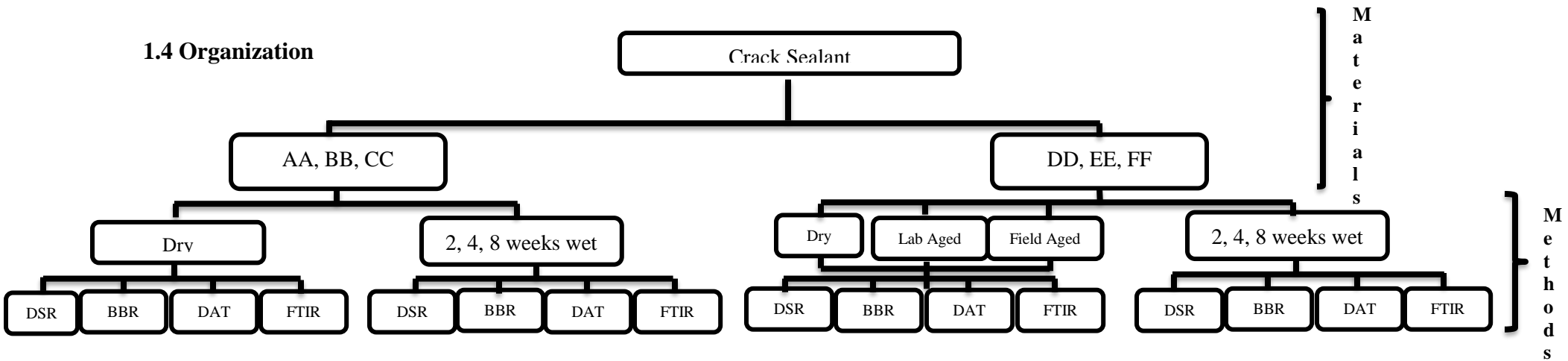


Figure 1. Experiment Plan

## **Chapter 2**

### **Literature Review: Crack Sealant and Asphalt**

Crack sealant is widely used to protect road pavement from damage caused by traffic and by water intrusion in the sub-layer. The two main types of crack sealants are the hot-poured and the cold-poured; they are used in various situations. However, the hot-poured is the most-used type of crack sealant, due to its flexibility after drying (Alpha Paving, 2016). Asphalt is also widely used for road pavement, and has been around for centuries. An investigation of virgin bitumen using atomic force microscopy shows the presence of “bee” structures. Researchers believe that the bee size influences the asphalt’s performance.

#### **2.1 How to Select Crack Sealant and Asphalt**

Choosing the right sealant for each pavement is very important. Researchers have studied the feasibility of using both hot and cold sealants. Different results, findings, conclusions, and recommendations were proposed, based on a two-year field-test survey. Four hot sealants and three cold sealants were chosen for the study. After eighteen months of field and laboratory investigation, it was found that the hot-poured sealants had excellent performance, in contrast to the cold-poured sealants, which showed a drastic decline in their performance with time (Yetkin et al., 2003). In addition, it was shown that hot-poured sealants got much less than cold-poured, and sealants with higher softening points performed better in higher temperature ranges.

Sealants are subject to shear forces during vehicles’ acceleration, and when light or heavy vehicles stop. In addition, cold urban conditions can significantly limit the number of sealant materials that perform well over many years (Masson et al., 1999). Selecting a sealant based on specific local needs such as climate conditions is crucial for pavement performance. Al-Qadi and

coworkers (2009) developed a modified testing method for performance-based guidelines for hot-poured bituminous crack sealant. It has been reported that using a double thickness in the standard BBR would overcome the excessive deflections during testing of crack sealant.

An investigation of virgin bitumen and recycled asphalt bitumen was conducted by Santos et al. (2015). Soft bitumen was reported to have larger bee structures and therefore a rougher surface; hard bitumen presented smaller bees and lower surface roughness. Furthermore, aging soft bitumen leads to an increase of the complex modulus and a decrease of the phase angle (Masson et al., 1998). The same properties were observed on recycled asphalt concrete.

An investigation of the microstructure features of bituminous binders by Fisher et al. (2013) shows the presence of the catana, the para, and the peri-phase. Further studies indicate that a softer bitumen displays a higher transition temperature of the peri-phase and vice versa (White et al. 2009). Considering that many studies have reported the presence of the “bee-like” features only on the binder surface, Fisher et al. (2013) also reported the presence of the catana-phase in the bulk property of the binder. They also showed that research conducted by Masson et al. (2006) describing the para-phase as being parallel to the peri-phase is in contrast to a continuous phase separating the peri-phase area.

## **2.2 Performance of Crack Sealant and Asphalt**

Cracking in pavements is almost an inevitable phenomenon. Cracking allows moisture to penetrate underneath the pavement layer, causing accelerated pavement deterioration (White et al., 2009) Sealant is widely used to fill cracks during pavement preservation. However, choosing the right sealant to extend the pavement service life is crucial. Yildirim and coworkers have conducted research on the service life of crack sealant used in Texas. The result shows that the cold-poured sealant has a service life of 10-16 months. While the hot-poured sealant

demonstrates a service life of 26 to 42 months. According to the Indiana Department of Transportation, four million dollars are spent annually on joint and crack sealing. Fang and coworkers investigated the cost-effectiveness of joint/crack sealing in relation to pavement performance. They concluded that there was no significant difference between the performance of sealed and unsealed sections regardless of pavement type, drainage conditions, and road classification (Fang et al., 2003).

Most researchers focus on developing performance-based specifications for bituminous sealants applied to asphalt concrete roadways and runways. It has been reported that joint and crack sealants used in airport pavement fail rapidly during cold climates, due to the lack of proper indications of the crack sealants' specification (Lacasse and Masson, 2004). Lacasse and Masson developed a performance-based specification for cold-applied joint sealants for Portland cement concrete. The specifications developed have shown a reduction of airport pavement maintenance cost, assisted in selecting joint sealants for very cold climates, and demonstrated extension of Portland cement concrete pavement service life.

An investigation of the chemical properties of asphalts and their relationship to pavement performance was conducted by Robertson (1991). It was found that the polarity among asphalt molecules varies widely, and the physical properties are governed by the balance of polar and non-polar (Masson et al., 1999). It was also reported that polar causes dissociation. In addition, excessive structuring leads to brittle cement that tends to crack; too little structuring leads to materials that deform under stress. Furthermore, the exact nature of the chemical bitumen is less important than the distribution of charge within the specific molecule.

Edwards and Redelius (2003) studied the rheological effects of adding two bitumen waxes: non-waxy and waxy. The result showed that the magnitude and type of effect on bitumen



rheology depend on the bitumen and type of crystallizing fraction in the bitumen. The DMA used for the study showed stiffening below 50°C for waxy bitumen but not for non-waxy bitumen. It has been reported that the presence of slack wax in bitumen negatively affects the bitumen by lowering the complex modulus at temperatures over 40°C (Masson, 2014).

## **2.3 Test Methods for Crack Sealant and Asphalt**

It is difficult to evaluate a crack sealant's performance using a laboratory test that accurately represents a field test (Ashok et al., 1997). Selecting an appropriate sealant is very important for the long-term performance of placements. It has been reported that most sealant selections are based on ASTM standards, not on performance indicators. A vacuum aging test to stimulate sealant weathering, a DSR test to assess tracking resistance, a BBR test to measure stiffness in low temperature, a t-bond strength test, and a blister test to measure sealant adhesive were proposed as guidelines for sealant selection (Al-Qadi et al., 2008).

Moreover, the effects of water, temperature, and humidity on the asphalt binder bee structures were investigated using atomic force microscopy (AFM) and Fourier transform infrared spectroscopy (FTIR). A sample was submerged in deionized water for eight days to see the water effect; and another sample was wetted with deionized water and placed in a tightly-closed jar for eight days. The AFM shows distinguished bee-like structures on the dry sample. However, the sample exposed to deionized water showed a decrease in the bee surface area that seems to disappear over time. Moreover, the AFM indicated the presence of nano-bumps, and the FTIR indicated a small amount of water absorbed (Goodwin et al., 2015).

### **2.3.1 Adhesion test**

The work of adhesion represents the energy required to separate two materials at the interface (Fini et al., 2011). Many states used crack sealants to prevent water from entering into

the lower structural layers of pavement, thereby extending its service life (Al-Qadi & Fini, 2013). It has been documented that the field performance of a crack sealant is determined by the properties and strength of the sealant-aggregate interface (Fini et al., 2011). Fini and coworkers measured and predicted the adhesion of hot-poured sealant to aggregates of different chemical composition. They have reported better adhesion for a crack sealant made of limestone compared to one made of quartzite. Moreover, it was reported that as the sealant surface tension decreases, its adhesion strength increases.

Sealant adhesion failure usually occurs due to a combination of multiple factors. The most common reason for sealant failure is excessive crack movement due to thermal expansion and contraction, wind loading, moisture-related movement, and differential thermal movement (Masson et al., 1998). It has been reported that wide cracks and joints can promote formation of a secondary crack. It has been shown that some causes of sealant failure are related to inadequate or imprecise description of the sealant's elongation and modulus properties.

It has been reported that limestone shows better adhesion to hot-poured binders than quartzite does. Fisher et al. (2012) investigated the interaction between the binder and several mineral surfaces, and reported that the peri/catana-phase shows good wetting due to adsorption of asphaltene aggregates to the mineral surfaces. They also used an atomic force microscope to determine the contact angle between the mineral surface and the micro-phases of bitumen. Considering that a smaller contact angle refers to strong adhesion bonding, the catana/peri-phase demonstrated a good wetting of the mineral surfaces in mica, calcite, and quartz glass; contrary to the perpetua-phase (Yetkin, 2002).

Fisher and Dillingh investigated cracks and healing on aged and unaged bitumen. It was found that the catana or bee-phase has a high modulus but low adhesion force compared to the

peri-phase, which displays a high modulus with small deformation and energy dissipation. An increase of the strain on the short-term aged bitumen shows a quick recovery of the crack surface. The quick recovery is due to the perpetua-phase that flows into the crack, closing the damage (Fisher et al., 2015). However, an increase in strain on a long-term aged bitumen results in holes that develop into cracks from the edges of the peri-phase.

### **2.3.2 Sessile drop test**

Determining a contact angle of a small droplet from a sessile drop has always been challenging. It has been reported that the most common technique to determine a static contact angle is to measure the height as a function of distance from the apex, which is followed by deriving a curvature either analytically (by fitting a straight line to the slope, if the drop is at the contact angle) or numerically (by integrating the Laplace-Young equation). It has been reported that most techniques become inaccurate or impractical for a small contact angle, making a sessile drop difficult to be observed in profile. Allen determined a small contact angle using two techniques: the small slope solution, where a sessile drop is assumed to be isothermal, so there is no variation in surface tension; and the spherical cap solution, where the shape of a sessile drop is assumed to be a spherical cap (Allen, 2003).

The surface displacement caused by a sessile drop could be very small for stiff solid surfaces, while significant for highly deformable substances and gels (Pozrikidis, 2013). It has been reported that there is a small change of the contact angle for a stiff solid surface, and highly deformable substrates cannot withstand capillary force. Researchers have determined a technique to prevent the physical deformation of a state at the contact line due to a sessile drop. They spread the capillary force over a strip with molecular or higher dimensions and used a sealing argument to show that the maximum vertical displacement of the contact angle is in order

(Pozrikidis, 2013). In addition, they also used another technique where they argued that plastic stresses developing near the contact line restrain the infinite deformation.

### **2.3.3 Dynamic shear rheometer test**

It has been documented that field study, which is the most reliable method to evaluate sealant performance in cold climates, is not a cost-effective method (Haithem and Shalaby, 2007). Researchers verified the laboratory tests used to characterize the hot-poured sealants in cold climates. They documented the dynamic shear rheometer (DSR) test and the cyclic and compression test as reliable laboratory methods that can replace costly and time-consuming field studies. Moreover, they also documented their methods as reliable to use for distinguishing poorly performing sealants.

Lu and Redelius (2006) studied the rheological effect of bitumen waxes and the impact of bitumen wax on asphalt mixture performance characteristics. It was shown that the rheological properties of bitumen at high service temperature, in most cases, are not influenced by wax content. It was also found that the difference in rutting between waxy and non-waxy bitumen was relatively small (Lu & Redelius, 2006). Moreover, the presence of wax in bitumen results in physical hardening, leading to asphalt mixtures with higher fracture temperatures.

### **2.3.4 Atomic force microscopy test**

De Moraes et al. (2009) studied the “bee” morphology at high temperature using AFM. It was observed that the shape and distribution of the bee phase depend on the temperature, time, and the heating history of the sample that was submitted. It was reported that the bees’ maximum height varies between 20-40 nm and 5-10 nm for a sample heated from room temperature up to

50°C (De Moraes et al., 2009). Further heating of the bitumen showed the disappearance of bees at temperatures higher than 70°C, and they begin to nucleate upon cooling to 66°C.

The effect of water on the microstructures of bitumen was investigated by Santos et al., and it was reported that the annealed bitumen showed nano-bumps on the film surface, in contrast to the non-annealed bitumen that didn't show any. Further investigation of different annealed bitumens showed the presence of nano-bumps in the peri- and catana-phases, but not in the para-phase, indicating that there are chemical and/or mechanical property differences between the para- and peri-phase (Santos, 2014).

## **Chapter 3**

### **Methodology**

#### **3.1 Materials**

The crack sealants used in this study were hot-poured sealant. The DD, EE, and FF crack sealants were provided by the Illinois Center for Transportation. The AA, BB, and CC crack sealants also used for the experiment were provided by CRAFCO, Inc., 6975 W. Crafcow Way, Chandler, AZ 85226 (<http://www.crafco.com>). The CC sealant is a hot-applied asphalt-based product from CRAFCO. It is a combination of Type II and Type III crack sealants; it is commonly used between the joints for low- and high-temperature weather, mainly because it remains ductile for a large temperature range. Sealant AA is mainly used in parking lot pavement and on highways, streets, and airfields (Crafco, 2008). Sealant BB is also an asphalt-based product that is mainly used to seal cracks and joints in cold to very cold climates, due to its softness (Crafco, 2010).

The asphalt binder used in this study was graded as a PG 64-22, which is commonly used in the United States and was donated by Associated Asphalt Inc. in Greensboro, NC. The wax that was used for asphalt binder modification was a paraffin wax with the catalog number P31-500. The wax was blended at 1%, 3%, 5%, and 10% wax by weight of the initial unmodified asphalt binder. Samples were hand-blended at 135°C for 30 minutes.

#### **3.2 Test Methods for Crack Sealant**

To better simulate the aging process that occurs in the field, an aging method was designed for the AA, BB, and CC crack sealants, and was compared with the DD, EE, and FF field-aged and lab-aged crack sealants. The field-aged and lab-aged crack sealants were received

from the University of Illinois at Urbana-Champaign. The field-aged crack sealant was collected from the field during resurfacing, two years after installation. The lab aging was done using vacuum-oven aging. The process was done by cutting the sealant into slices and placing 35 g into a stainless steel pan. The pan was then transferred into a conventional-controlled oven at 180°C for five minutes to melt and form a thin film. Next, the sealant was removed and allowed to cool at room temperature before placing it into a preheated vacuum oven at 115°C for 16 hours. Finally, after 16 hours, the sealant was transferred back into the conventional-controlled oven at 180°C for five minutes or until the sealant was fluid enough to pour (Al-Qadi et al., 2009). The other aging method was used on the AA, BB, and CC crack sealants. The aging was done by first cutting small pieces of sealant and placing them into a can. The can was heated at 185°C for 30 minutes in a conventional-controlled oven. Then 35 grams of the sealant was poured into a stainless steel pan and placed into the oven at 150°C overnight to represent harsh weather. Next, the sealant was removed from the oven and poured into a DSR mold, allowed to cool at room temperature, and transferred into a water bath at 40°C for two weeks to represent rain, before testing.

### **3.3 Sessile Drop Methods and Contact Angle**

A sessile drop test is the analysis of a drop of target liquid on a solid substrate. The components of sessile drop equipment are a light source, sample stage, lens, and image-capturing tools. The contact angle can be measured directly by examining the angle formed between the solid and the tangent to the drop surface (Figure 2). The contact angle is defined as the angle between the tangent to the liquid-fluid interface and the tangent to the liquid-solid interface (Marmur, 2006). It has been reported that a contact angle less than 90°C indicates that wetting of the surface is favorable, so the liquid will spread over a large surface area; a contact angle greater

than 90°C indicates that wetting of the surface is unfavorable, so the liquid will minimize its contact with the surface (Young and Lee, 2013). So a smaller contact angle indicates that the bond between the substrate and the liquid is most likely not to fail in adhesion; and a bigger contact angle indicates the likelihood of the bond between the substrate and liquid to fail in adhesion. The instrument used to determine the contact angle was the First Ten Ångstroms (FTA-1000 model) designed by Dr. Roger Woodward. That machine operates by taking an image of a drop on a camera and analyzing the captured image on a personal computer. The sessile drop method was used in this study to measure the contact angle between water and sealant. The calculation of the contact angle was done by using the Young-Laplace equation (Yuan and Lee, 2013):

$$\gamma_{lv} (\cos \theta_Y) = \gamma_{sv} - \gamma_{sl}$$

where:

$\gamma_{lv}$  = liquid-vapor interfacial tension

$\gamma_{sv}$  = solid-vapor interfacial tension

$\gamma_{sl}$  = solid-liquid interfacial tension

$\theta_Y$  = Young's contact angle

Figure 2 shows an image of the FTA instrument and an image of a sessile drop. Prior to testing the contact angle with sealant, water and the sealant surface were heated in the environmental chamber at temperatures ranging from 40°C to 80°C. Those temperatures represent pavement surface temperatures in a hot summer season. The solid surface, in this case the sealant, was prepared by melting the sealant in the oven at 185°C for 30 minutes, then slowly pouring it into aluminum molds to form a flat and smooth surface. The aluminum molds were cooled at room temperature for one hour, and then placed on the FTA-1000 tray. Water at different temperatures was inserted into the syringe and placed inside the FTA-1000 chamber so



the temperature could remain constant during measurements. Finally, the contact angles of six droplets were evaluated for each water droplet at three sealant surfaces.

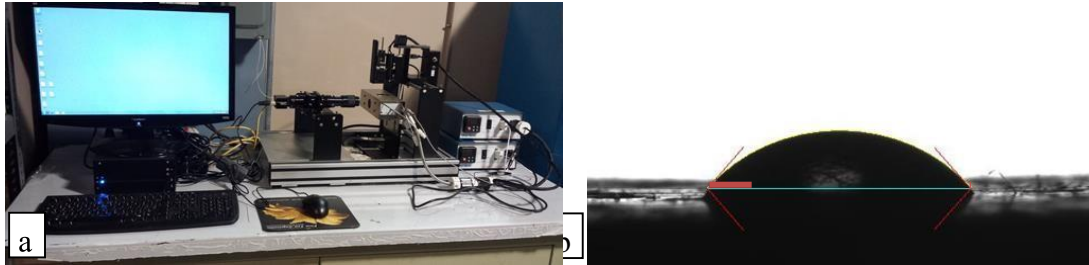


Figure 2. (a) FTA-1000 and (b) image of a droplet of water on sealant surface

Table 1. Crack Sealants and Properties

Sealant	Application Temp. (°C)	Maximum Temp. (°C)	Application Climate	Viscosity at 190°C (Pa.S)	Flow at 60°C	Resilience, %	Cone Penetration at 25°C
Crafco Type I	193	204	Warm to hot climates	4783	5.0 max	N/A	90 max
Beram 195 (Type II & III)	185	200	Moderate climates	3483	3.0 max	60 min	90 max
Crafco Type IV	177	204	Cold to very cold climates	1354	3.0 max	60 min	90-150

### 3.4 Asphalt Test Methods

Using the rotational viscometer (RV), the viscosity results were determined. Measurements were conducted following ASTM D4402, using a Brookfield Viscometer RV-DVIII Ultra by applying a rotational shear on the selected material. Test specimens were prepared by pouring 10.5 grams into a specific aluminum chamber, then allowing it to cool to room temperature. Samples were preheated in an oven for 30 minutes before being placed into the temperature-controlled thermostat. After thermal equilibrium was reached, three viscosity results were taken at three-minute intervals until the results had a range of less than 100 cP (0.1

Pa\*s). The average of these three numbers was taken as the true value. The speeds chosen for this study were 20 rpm and 50 rpm, performed at 105, 120, 135, and 150°C.

The DSR was used to investigate the elastic and viscous behavior of wax-modified asphalt binder by measuring the resulting shear stress and shear strain, which when divided gives the complex modulus ( $G^*$ ) of the material.  $G^*$  is typically defined as the measure of a binder's resistance to deformation when repeatedly sheared. In order to determine  $G^*$ , 31 different oscillations were applied to the sample, ranging from 0.1 rad/s to 100 rad/s, at 11 temperatures ranging from 70°C to 4°C. For temperatures from 70°C to 52°C, the 25 mm spindle was used, while the 8 mm spindle was used at temperatures from 46°C to 4°C. From the resulting data, master curves were generated using the principle of time-temperature superposition (TTS) at a reference temperature of 36°C.

Atomic force microscopy (AFM) was used to further examine the results of calculations in a real laboratory setting and examine the overall asphalt structures and morphological characteristics of asphalt in the presence of various percentages of paraffin wax. To do so, specimens were prepared on glass microscope slides that were cut into squares (0.5×1 inches) and cleaned by ultra-sonication in acetone, followed by isopropanol and then water. Paraffin wax (P31, with melting point of 53°C -57°C, acquired from Fisher Scientific) was added to PG 64-22 bitumen (acquired from Associated Asphalt Inc.) in different weight percentages of 0% to 10% relative to the weight of the base bitumen.

Differential scanning calorimetry (DSC) was used to determine the heat capacity and the glass transition temperature ( $T_g$ ), and to illustrate the effect of wax on binder properties. The heat capacity was determined by the three-run method, and the glass transition temperature ( $T_g$ ) was determined by MDSC in heating. The three-run heat capacity approach uses an isothermal –

ramp – isothermal DSC method. This method consists of empty pans, the sample, and reference materials such as sapphire. The empty pan baseline was subtracted from the reference results to determine a conversion factor of heat flow (mW) to heat capacity ( $J/^\circ C$ ). Then the heat flow difference between the sample and the empty pan baseline is determined, divided by the sample mass, and converted to heat capacity ( $J/g^\circ$ ) using the conversion factor. Replicate heat capacity determinations using the three-run method typically agree within about 3% or less. The test started at  $-80^\circ C$  to  $150^\circ C$ . The samples (5-7 mg) were placed in T0 aluminum pans with hermetic lids.

The bending beam rheometer (BBR) was used to determine the modified binder's stiffness and m-value at low temperature. For the low temperature testing,  $-12^\circ C$  was selected, since it is typically the rule to test the binder at the PG grade of the neat binder plus  $10^\circ C$ . Samples were prepared by heating the samples to liquid status, then pouring them into aluminum molds. The binder was allowed an hour to cool to room temperature; then it was placed into a freezer for five minutes before being demolded. After being demolded, specimens sat at room temperature for two minutes before being placed into the BBR testing chamber for exactly one hour; then they were tested.

The Direct Adhesion Test (DAT) was conducted by applying tensile force on a sealant-substrate interface. In this test, the mold assembly consists of two aluminum half-cylinders of 25mm diameter and 12mm length. The assembly has a half-cylinder mold, open at the upper part. Prior to pouring the bitumen, the assembly was heated to facilitate asphalt flow and to ensure a uniform bonding area (Figure 3). A pre-debonded area was formed using a thin shim in the form of a notch at the upper edge of the interface; this shim was placed at one side of the assembly to ensure adhesive failure as well as to pre-define the failure path. The waxy asphalt

binder adhesion strength (peak load before failure) and fracture energy (energy required to break the bond) were measured. The specimens were slowly poured into adhesion molds to avoid trapping air bubbles. After 1 h of annealing at room temperature, the sample was trimmed and then placed into the DAT cooling bath at  $-12^{\circ}\text{C}$  for 15 min. Afterwards, each specimen was removed from the bath for demolding by removing the bottom tray as well as the metal shim; specimens were then placed back into the cooling bath for 45 min before testing.

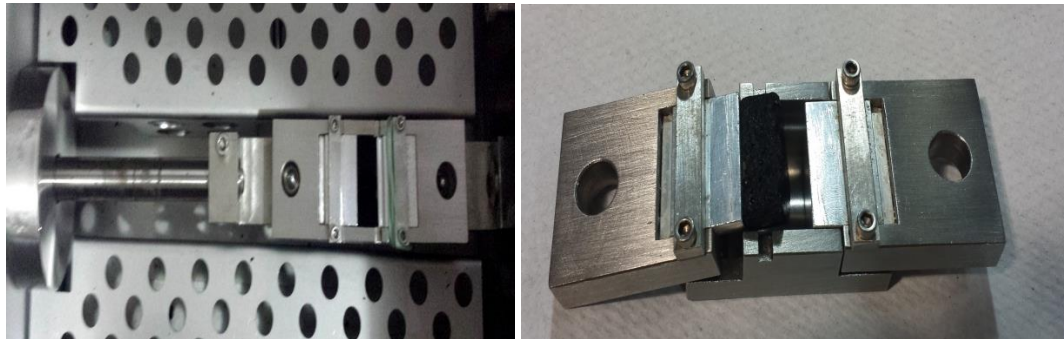


Figure 3. Direct Adhesion Test Fixture

The direct tension test is another low-temperature test to determine the properties of the modified binder. The testing apparatus applies direct tension to dog-bone-shaped asphalt-binder specimens. Samples were prepared according to ASTM D6723-12. The binder was heated to a liquid state, poured into defined aluminum molds, allowed to cool to room temperature for one hour, trimmed, placed in a freezer for seven minutes, and finally demolded for placement in the DTT methanol bath. Like the BBR and DAT methods, the testing temperature was  $-12^{\circ}\text{C}$ . Samples remained at  $-12^{\circ}\text{C}$  for exactly one hour to ensure thermal equilibrium. During the test, load and displacement of the sample up to failure is recorded then used to determine fracture energy (the amount of energy required to create two new surfaces) and ductility (the change in length divided by the original length).

## Chapter 4

### Results

#### 4.1 Dynamic Shear Rheometer Test

##### 4.1.1 Crack Sealant

To better simulate the aging process that occurs in the field, an aging method was designed for the AA, BB, and CC crack sealants, and was compared with the DD, EE, and FF field-aged and lab-aged crack sealants. The field-aged and the lab-aged crack sealants were received from the University of Illinois at Urbana-Champaign. The field-aged crack sealant was collected from the field during resurfacing, two years after installation. The lab aging was done using a vacuum-aging oven. The process was done by cutting the sealant into slices and placing 35 g into a stainless steel pan. The pan was then transferred into a conventional-controlled oven at 180°C for five minutes to melt and form a thin film. Next, the sealant was removed and allowed to cool at room temperature before placing it into a preheated vacuum oven at 115°C for 16 hours. After 16 hours, the sealant was transferred back into the conventional-controlled oven at 180°C for five minutes or until the sealant was fluid enough to pour (Al-Qadi et al., 2009). The other aging method was used on the AA, BB, and CC crack sealants. The aging was done by first cutting small pieces of sealant and placing them into a can. The can was heated at 185°C for 30 minutes in a conventional-controlled oven. Then 35 grams of the sealant was poured into a stainless steel pan and placed into the oven at 150°C overnight, to represent harsh weather. Then the sealant was removed from the oven, poured into the DSR mold, allowed to cool at room temperature, transferred into a water bath at 40°C for two weeks to represent rain, and tested.

Figure 4. shows the relaxation time of the different types of crack sealants at different aging conditions. The field-aged samples have the highest relaxation time as expected, in

contrast to the aging method used on the AA, BB, and CC crack sealants. Since the aging time is far below the field-aged sample, it suggests that this aging method is not as severe as the aging method used for the DD, EE, and FF crack sealants; it represents only 56% of the field-aged. The vacuum-oven aging that was used for sealants DD, EE, and FF was close to the aging process that happens outside in the field. There is an increase in relaxation time almost similar to the field-aged. The DD crack sealant relaxation time was even higher than the one collected from the field; up to 87% of the field-aged is represented using that method. This shows that the vacuum-oven aging method would be the most appropriate method to simulate sealant weathering.

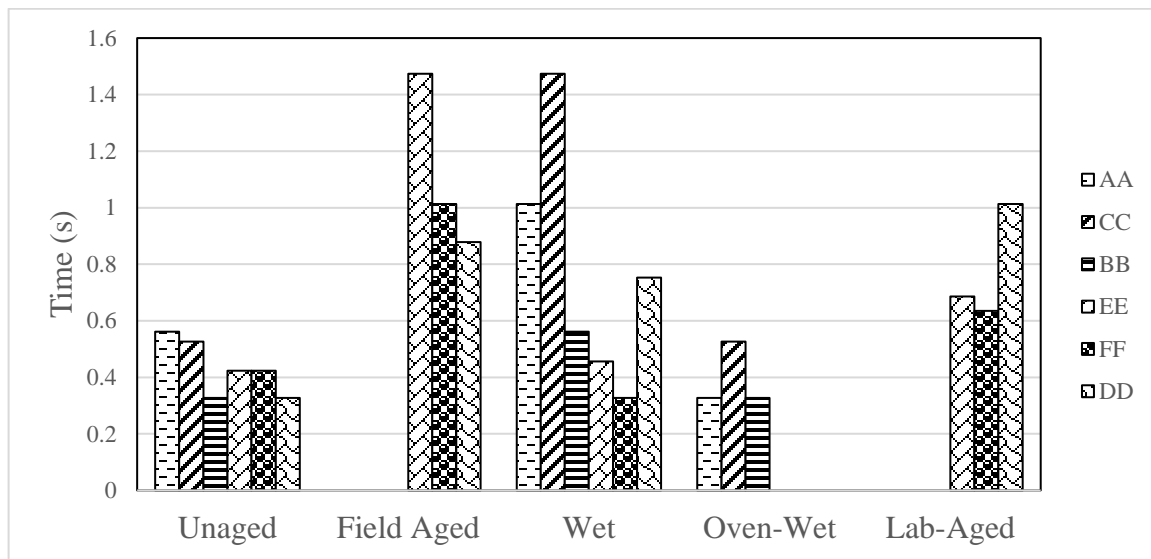


Figure 4. Relaxation Time for Different Aging Methods

#### 4.1.2 Asphalt

Using the dynamic shear rheometer (DSR), the generated master curves for 0%, 1%, 3%, and 10% wax are given in Figures 5a and 5b. In Figure 5a, the higher reduced frequency results indicate that increasing the wax percentage leads to a significant decrease in complex modulus, meaning that the binder is softer at this temperature range. At lower reduced frequency values, the difference does not appear to be as significant; however, with increasing wax percentage, the

complex modulus appears to show an increase in complex modulus, meaning that the binder is becoming stiffer in this range.

In order to investigate this phenomenon more closely using the DSR, the point at which the elastic and viscous modulus intersects was also determined. The point at which this happens is also known as the crossover temperature (Figure 5b), which can be described as the hardness parameter of the binder. The unmodified binder was shown to have a crossover temperature of 9°C. As expected, at 3% and 10% wax, the crossover temperature was shown to significantly increase 3°C and 25°C, respectively. However, unlike at 3% and 10%, at 1% wax, it is interesting to note that the crossover temperature was observed to decrease by nearly 1.3°C. Therefore, low-temperature characterization is needed to determine if this trend can be consistently observed.

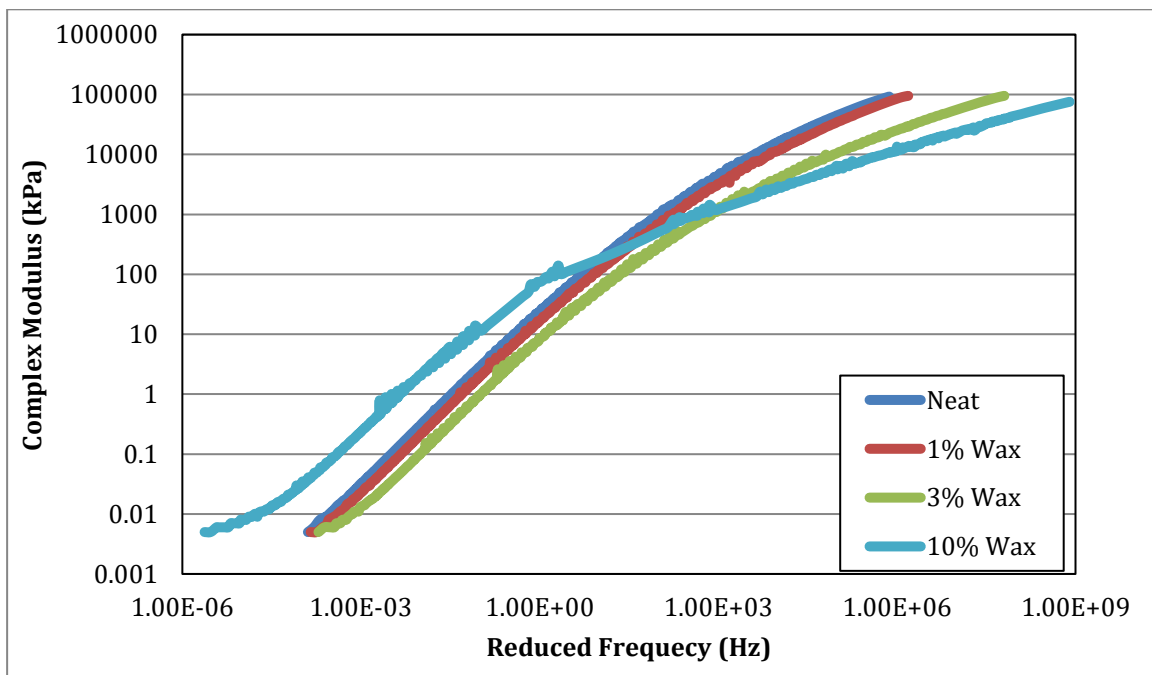


Figure 5a. Rotational Viscometer Results for 0%, 1%, 3%, and 10% Wax-Modified Binder

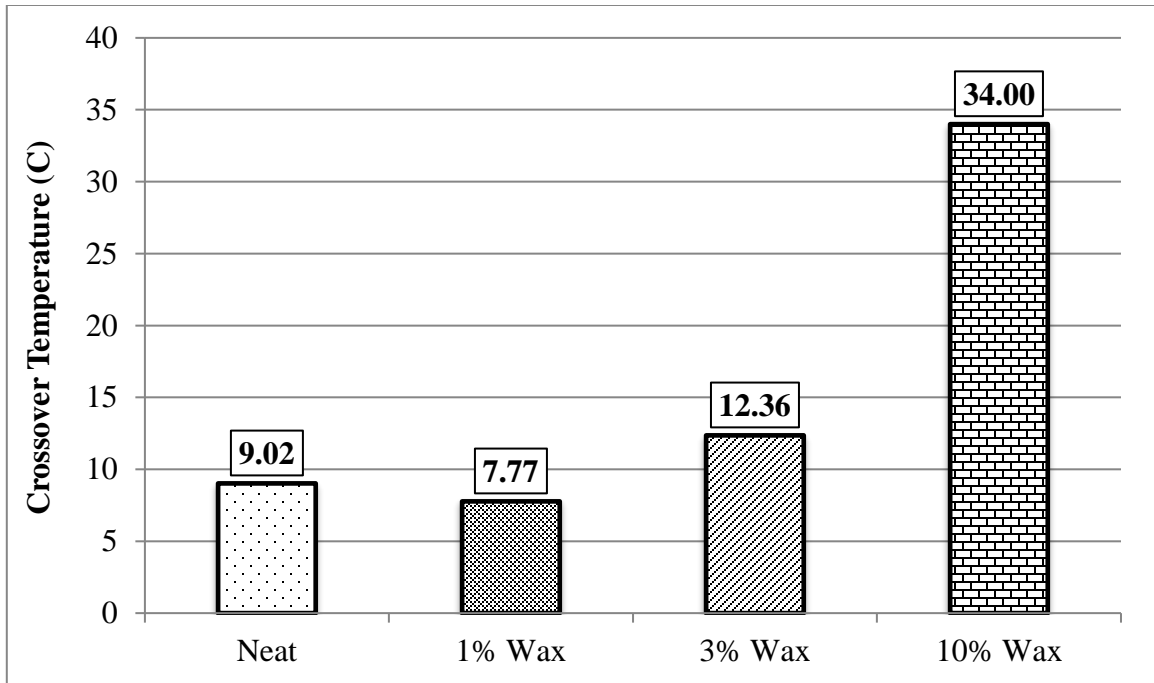


Figure 5b. Crossover Temperatures for 0%, 1%, 3%, and 10% Wax-Modified Binder

## 4.2 Relaxation and Modulus of Elasticity

### 4.2.1 Relaxation

When a constant displacement is applied on a viscoelastic material (such as a sealant) the stress is formed and is reduced as time passes. One of the basic models used to represent the viscoelastic material is the Maxwell Model which consists of a spring and a dashpot in series. The relaxation time in the Maxwell Model is  $T_0$ , which is the time required for the stress to reduce to 36.8% of the initial value (Yang, 2003). The shorter the time, the more rapid the stress relax. In this study the investigation of how water affects the crack sealant was performed based on the relaxation time measured using the DSR machine, and then was compared between the joint sealants. The sample was prepared by first heating the crack sealant at 185°C for 30 minutes, and then pouring it into the DSR mold. After one hour of curing at room temperature, the sample was placed into a control bath at 40°C and then tested after 2, 4, and 8 weeks.



Figures 6a - 6d show the relaxation time of all the crack sealants before and after 2, 4, and 8 weeks of water exposure. The graph shows a low relaxation time before conditioning, and an increase in relaxation time after conditioning. This increase in time could be due to water absorption by the sealant, changing its chemical properties. Figures 6b-d show that the CC, FF, and EE crack sealants from the virgin, lab-aged, and field-aged, respectively, have the highest relaxation time after conditioning, suggesting that it takes longer for the energy or stress to dissipate through the sealant after a load is applied. The other crack sealants show the same variation as well, but at a lower scale. However, the virgin BB crack sealant shows the lowest relaxation time after conditioning, indicating that the stress recovery improves over time.

More research has been done on how water affects sealants when exposed beyond two weeks, to examine whether the process reverses after a longer time. From Figures 6b - 6d, the relaxation time increases as the crack sealant is exposed to water for a longer time period (8 weeks). There is an increase of at least 59%, 46%, and 240% respectively for the virgin, lab-aged, and field-aged crack-sealant relaxation time. These increases indicate serious water damage after a few weeks of water exposure.

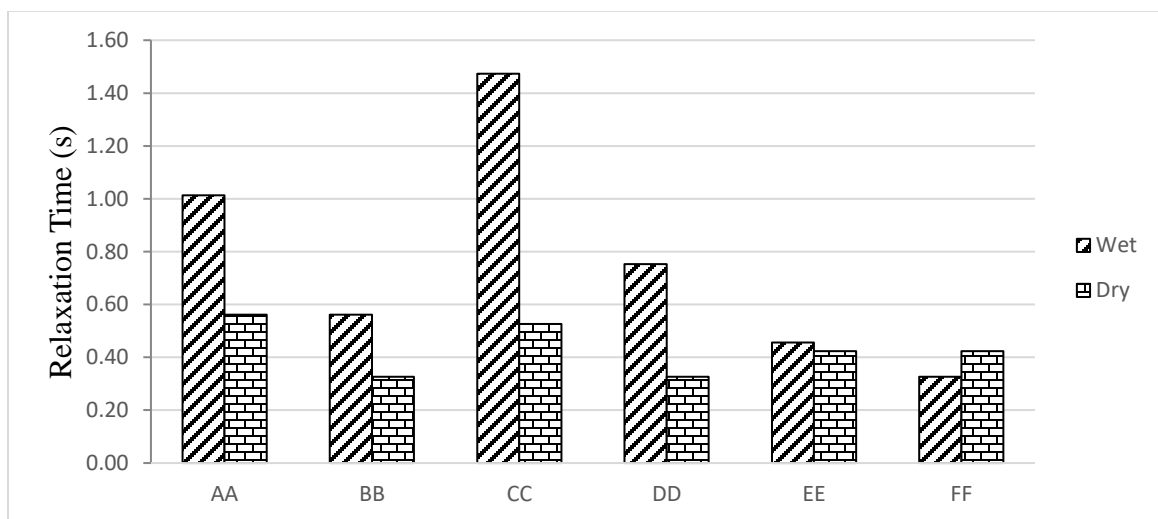


Figure 6a. Sealant Relaxation Time Before and After 2 Weeks of Water Exposure

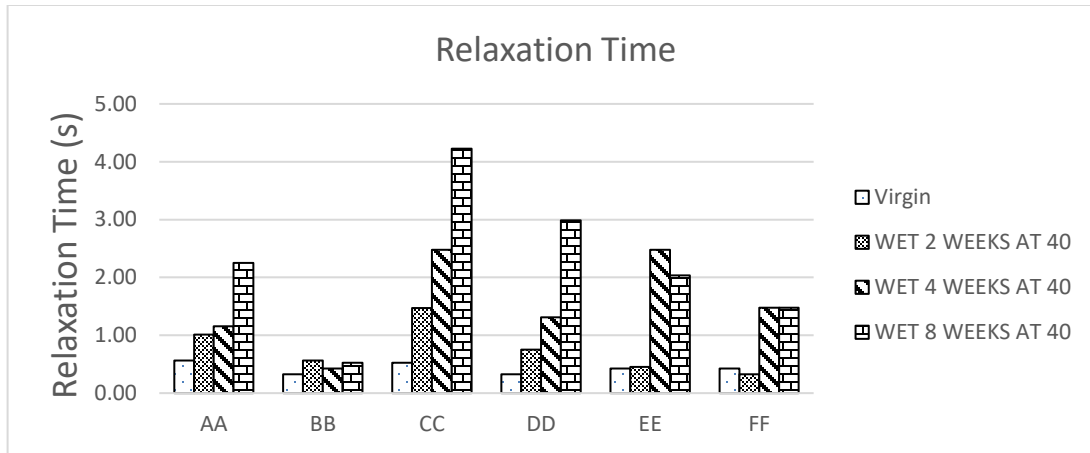


Figure 6b. Sealant Relaxation Time Before and After Water Exposure

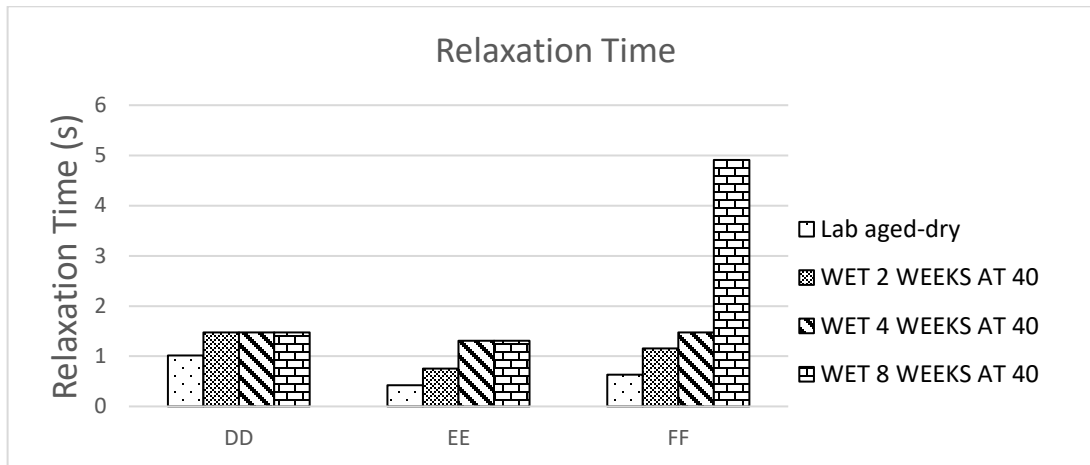


Figure 6c. Lab-Aged Sealant Relaxation Time Before and After Water Exposure



Figure 6d. Field-Aged Sealant Relaxation Time Before and After Water Exposure

#### 4.2.2 Modulus of Elasticity

The modulus of elasticity determines a material's ability to resist deformation; the higher the modulus of elasticity, the stiffer the material. The stiffer the sealant, the more stress and energy is formed inside the material. Reducing the dissipated energy helps improve the performance of the sealant material and therefore extends its service life. In this study, the modulus of elasticity is measured as an indicator of performance. The modulus of elasticity is measured in shear creep mode with a dynamic shear rheometer (DSR). The test used a 100% constant shear strain,  $\gamma$ , which means 0.08 radians ( $4.58^\circ$ ) was applied to the 25-mm diameter and 1-mm height (gap size) of the sample. Finally, the resulting shear modulus of elasticity was calculated for each crack sealant during the relaxation period. Figure 7 shows a decrease in the modulus of sealants DD, EE, FF, AA, CC, and BB after two weeks in water; this decrease in modulus is due to the effect of water on the sealants' rheological properties. As time increases, the sealant's physical properties are progressively weakened due to the water's effect, causing a decrease of the sealant's modulus of elasticity and making the sealant softer. A low modulus can be in favor of sealants, reducing stresses in the sealant and in the interface. However, the EE crack sealant that has spent two weeks in water has a higher modulus than unaged EE (Figure 7b). This could be due to the presence of water affecting this sealant's chemical properties. An increase in the modulus of elasticity could lead to a stiffer material that becomes brittle and breaks easily, causing a cohesive failure.

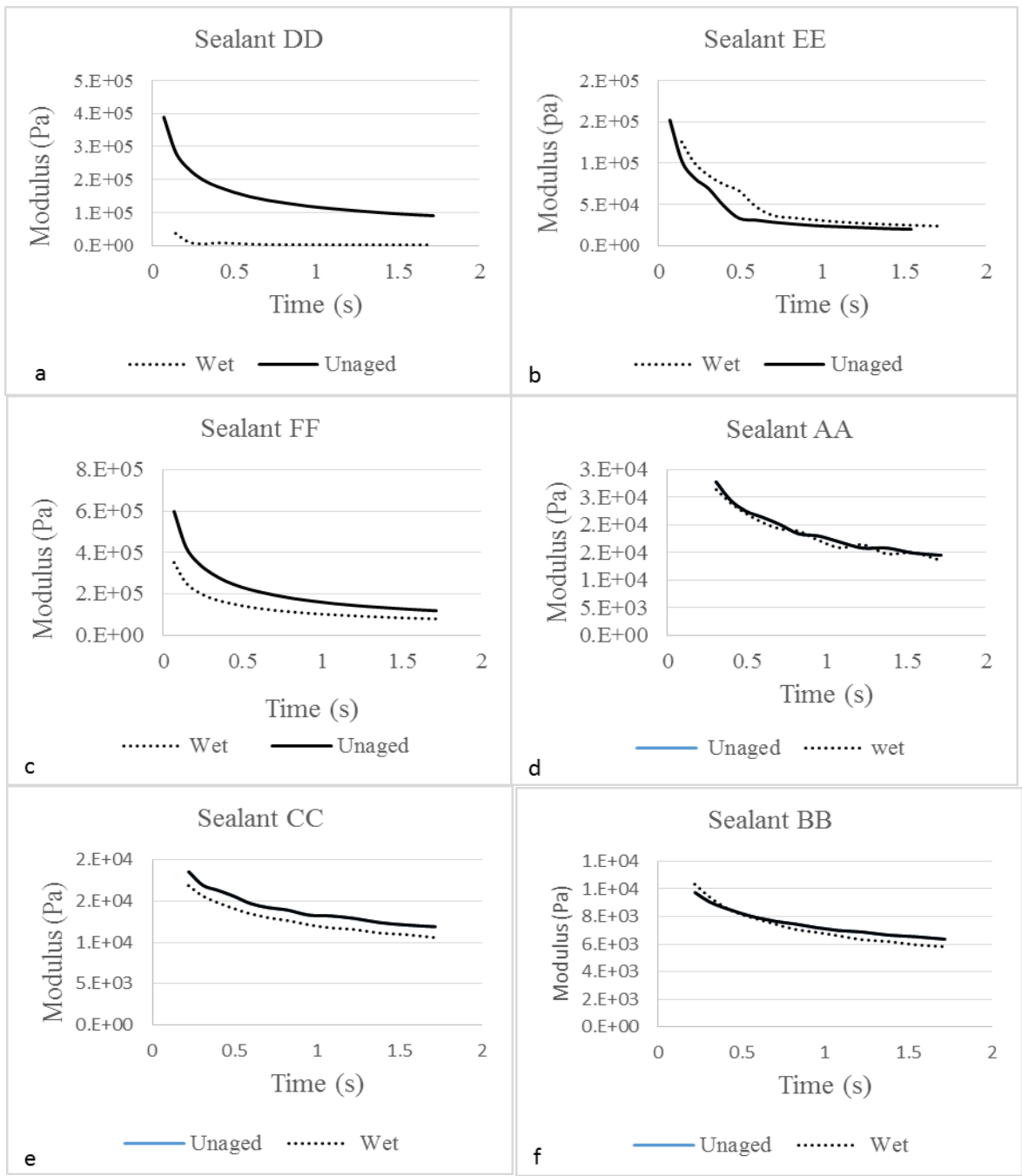


Figure 7. Sealants DD, EE, FF, AA, CC, and BB Before and After Water Exposure

## **4.3 Bending Beam Rheometer Test**

### **4.3.1 Crack Sealant**

To further understand crack sealants' susceptibility to cold water, the low-temperature stiffness and relaxation properties of the sealants were measured using an extended bending beam rheometer (BBR) test. In an extended BBR test, the beam has a height of 12.70 mm, twice the 6.35 mm height of the beam in the standard BBR test. A load of 980 mN is applied to the mid-span of the sealant beam for 240 seconds (creep duration). The load is removed from the sample, and the rebound of the mid-span is measured and captured for 460 seconds (recovery period). The extended BBR test was conducted on every sample at  $-12^{\circ}\text{C}$ . The data collected from the test shows an indication of the sealant's recovery capacity at low-temperature, the change in recovery parameter was used as a measure of sealant susceptibility to water. The creep/recovery test results were used to develop a measure of recovery. Figure 8a shows the peak deflection (A), which is the maximum deflection measured at the end of the creep period (240 seconds). The recovery (B) is the amount of deflection recovered during the recovery period and is measured at the end of the recovery period (700 seconds); the residue (C) is the amount of non-recovered deflection at the end of the recovery period. An increase in the recovery value or a decrease in the residue value indicates a better recovery.

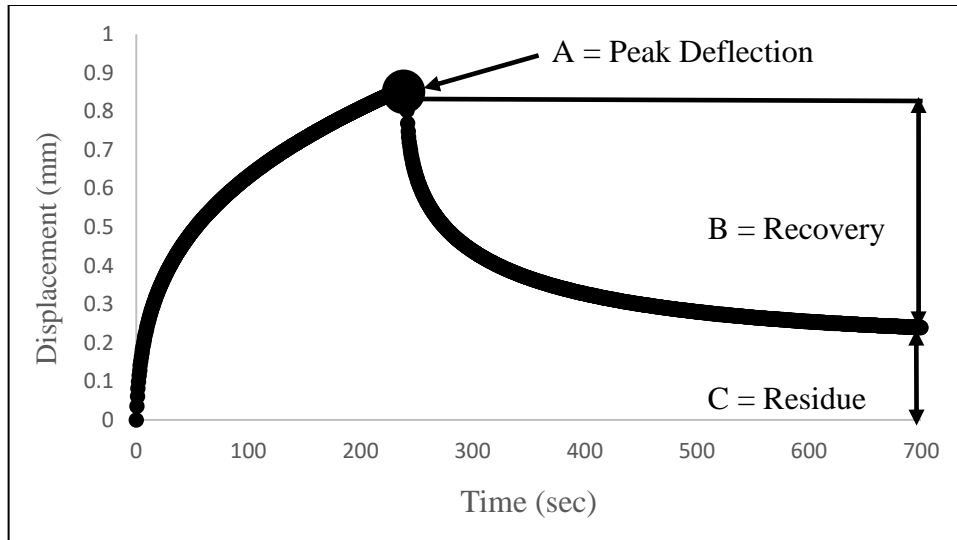


Figure 8a. Bending Beam Rheometer Illustration

Figure 8b shows the recovery of the DD and FF crack sealants after the load is removed. There is not much change in the recovery of the two crack sealants between the wet and dry. The DD and FF crack sealants, however, show a decrease in the residue after conditioning, indicating a faster recovery time. The recovery (Figures 8c and 8d) and slope (Figure 8e) at 50% were also determined. The recovery and slopes were not consistent for the two crack sealants. Unexpectedly, the dry sealant seems to recover more slowly than the wet sealant. This could be due to the fact that sealants DD and FF have better properties to resist a low-temperature climate. Sealant DD, however, shows a slower recovery after water conditioning.

Figure 8d shows an extended water exposure (up to 6 weeks) to better understand the effect of water exposure on crack sealant recovery. Sealants AA, BB, and CC show an initial decrease in recovery after having been exposed to water for 6 weeks; beyond 2 weeks of water exposure, there is an increase in recovery, indicating a better performance. The recovery shows an improvement at 6 weeks in the water for the AA and CC crack sealants. However, the BB crack sealant shows an improvement only after 4 weeks in the water. Overall, sealant CC has the

best recovery with 92% total recovery, followed by sealant AA with 57% and finally sealant BB with only 56%.

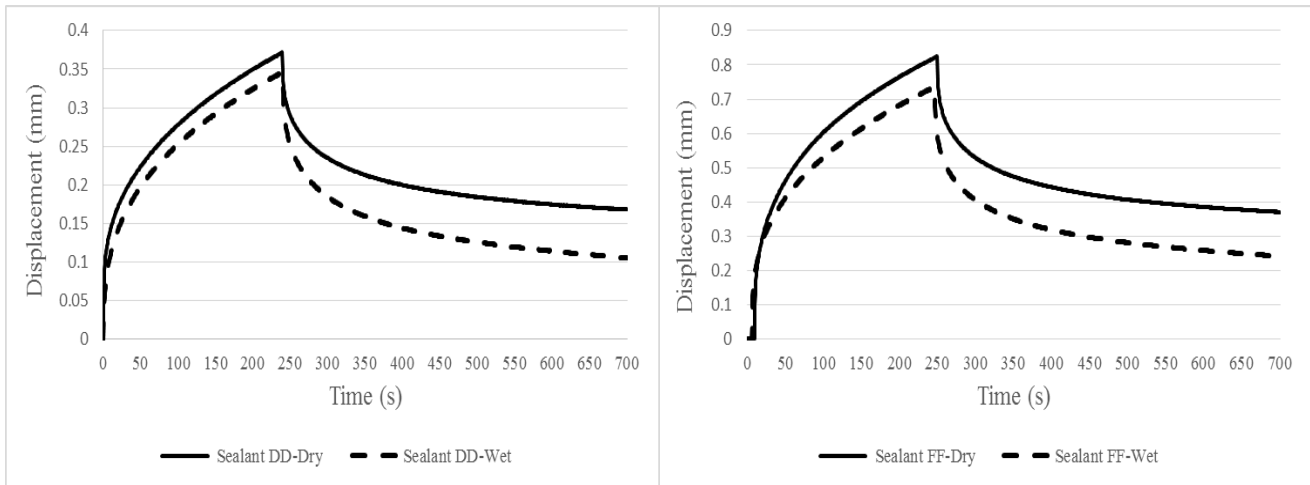


Figure 8b. Bending Beam Rheometer Test Before and After Water Exposure

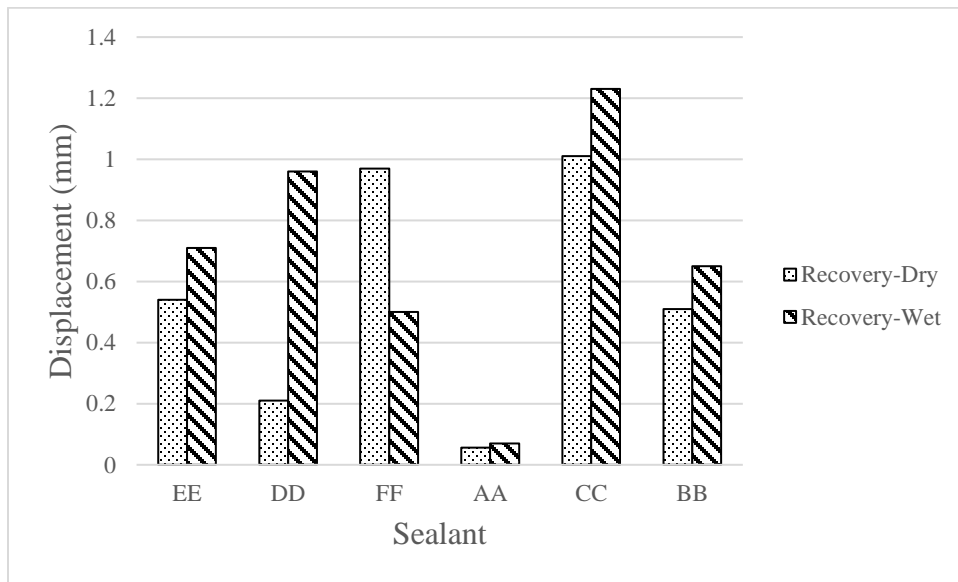


Figure 8c. Crack Sealant Recovery Before and After Water Exposure

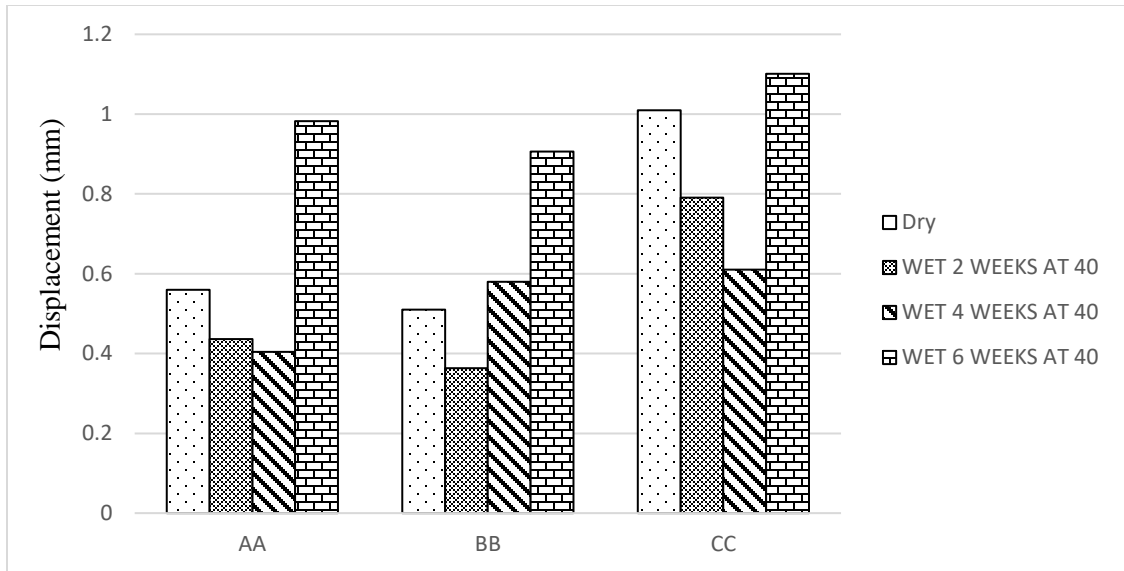


Figure 8d. Crack Sealant Recovery Before and After Extended Water Exposure

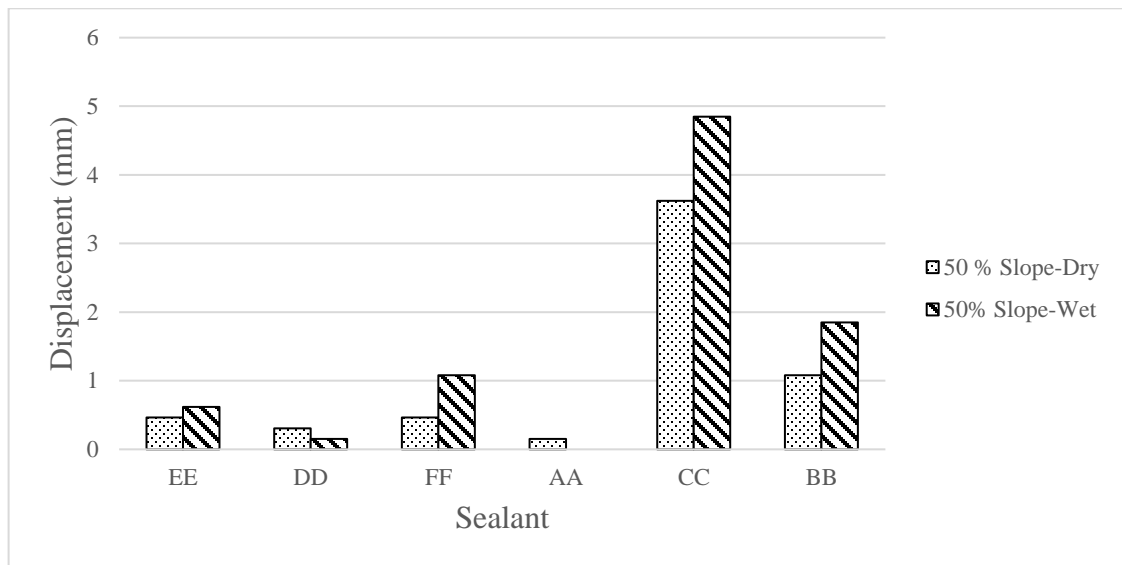


Figure 8e. Crack Sealant 50% Slope Before and After Water Exposure

### 4.3.2 Asphalt

Figure 9 shows the stiffness and m-value results that were determined using the BBR. The stiffness results (left axis) show that increasing the wax percentage leads to a higher stiffness value. This is consistent with the increased crystallization effect of the paraffin wax. This is also



shown with the modified binder's decreased ability to relax stress, as shown by the decreasing m-value results (right axis).

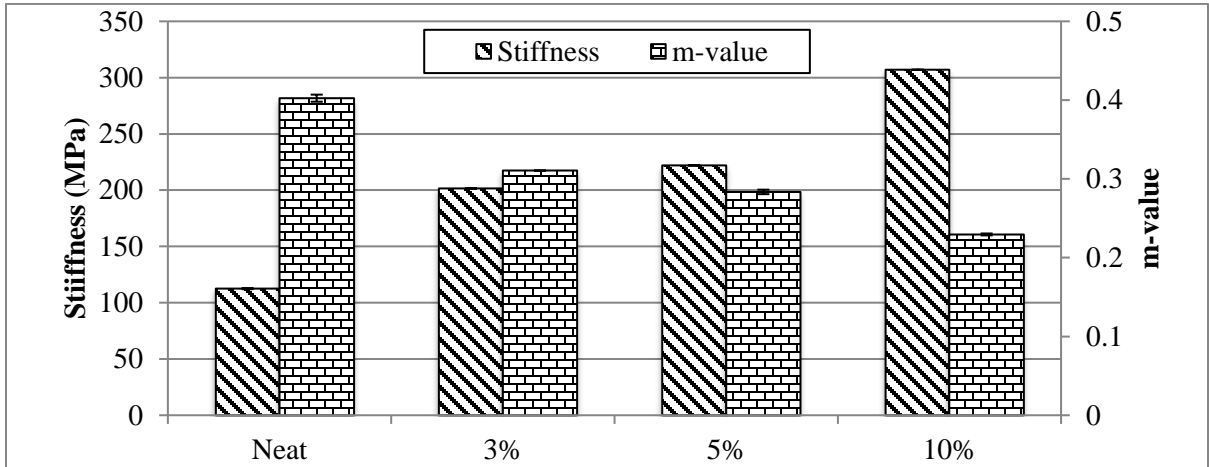


Figure 9. Stiffness and M-Value Results for 0%, 3%, 5%, and 10% Wax-Modified Binder

#### 4.4 Direct Adhesion Test

##### 4.4.1 Crack Sealant

A direct adhesion tester (DAT) was used to determine a sealant's adhesion failure before and after water exposure. The adhesion test was conducted by applying a tensile force on a sealant-substrate interface. The sealant's adhesion strength (peak load) and the fracture energy (energy required to break the bond) were measured before (dry) and after conditioning (wet) to examine the theory that the energy required to cause an adhesion failure decreases after water exposure.

Specimens were prepared by heating the sealant at 185°C for 30 min, then slowly pouring it into the adhesion molds to avoid trapping air bubbles. After 1 h of annealing at room temperature, the sample was trimmed and placed into the DAT cooling bath at -12°C for 15 min. After that, each specimen was removed from the bath for de-molding by removing the bottom tray as well as the metal shim; specimens were then placed back into the cooling bath for 45 min

before testing. The same procedure was performed for experiments under wet conditions, for which each specimen after de-molding was placed into a water bath at 40°C for 24 hours before placing it into the cooling bath in preparation for running the adhesion measurements.

As shown Table 2 and Table 3, there is a reduction in both peak load and energy after the sealant is exposed to water for 24 hours. Accordingly, it can be observed in Figures 10a and b that as the sealant is exposed to water, there is a loss of energy and a reduction of maximum load required to break the bond, indicating progressive alteration of sealant surface properties. The loss of energy between the substrate and sealant is due to water affecting the bond between those two by causing a change in surface properties. This in turn could lead to a loss of adhesion, leading to premature sealant failure. The results also showed that the reduction in adhesion strength varied depending on the sealant type. The AA crack sealant showed little change in energy and minimal peak load reduction; the CC and BB crack sealants showed a significant loss of energy after conditioning. This is due to the fact that the CC and BB sealants have a low modulus of elasticity, suggesting they stretch less than other crack sealants; therefore, the sealants' change of surface structure due to water exposure will lower their modulus of elasticity and decrease the energy required to break the bond. In addition, the substrate used for the study was an aluminum, which has no porosity, compared to a substrate with a rough surface that gives something to grip, producing a stronger bond. Furthermore, the DD and FF crack sealants displayed a higher amount of energy after conditioning. This could be due to the fact that they have a high modulus of elasticity, suggesting they stretch more, especially at low temperatures, therefore requiring more energy to break the bond they form with the aggregate.

Table 2. Direct Adhesion Load Test Results Before and After Water Exposure

	Load (N)		COV (%)	
	Dry	Wet	Dry	Wet
<b>CC</b>	17.4	12.0	0.05	0.15
<b>AA</b>	27.8	26.6	0.13	0.09
<b>BB</b>	11.1	10.7	0.00	0.03
<b>EE</b>	18.9	19.9	0.09	0.12
<b>FF</b>	30.7	22.4	0.02	0.10
<b>DD</b>	31.2	43.4	0.07	0.04

Table 3. Direct Adhesion Energy Test Results Before and After Water Exposure

	Energy (J)		COV (%)	
	Dry	Wet	Dry	Wet
<b>CC</b>	115.2	17.30	0.30	0.82
<b>AA</b>	4.9	3.9	0.30	0.04
<b>BB</b>	68.3	22.3	0.00	0.16
<b>EE</b>	97.8	90.1	0.15	0.12
<b>FF</b>	90.5	101.8	0.21	0.21
<b>DD</b>	14.9	98.4	0.29	0.60

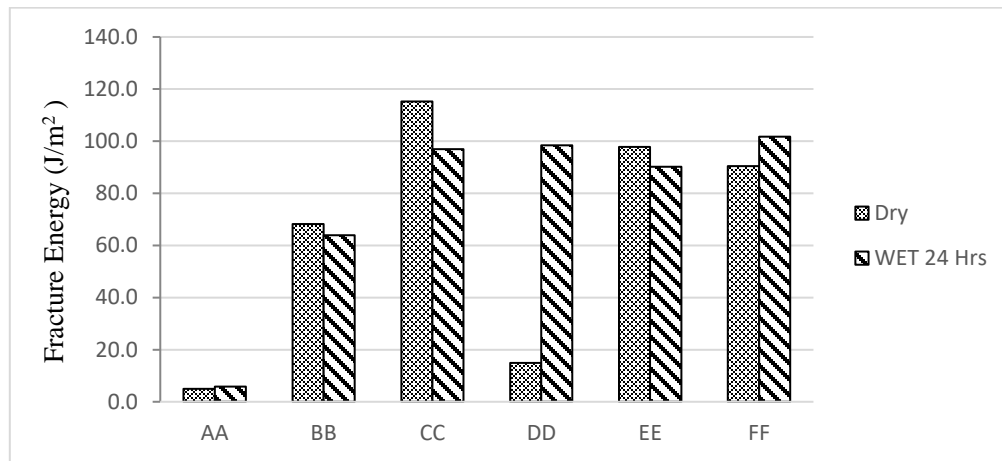


Figure 10a. Fracture Energy Before and After 24 hours of Water Exposure

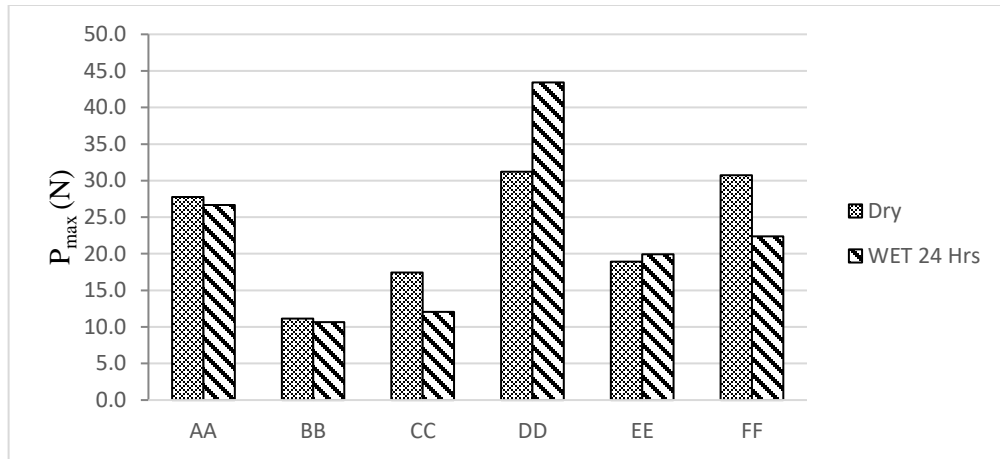


Figure 10b. Peak Load Before and After 24 hrs Water Exposure

#### 4.4.2 Asphalt

The adhesion strength of wax-modified binder was measured using a DAT test that measured load and displacement as a function of time; the collected data were then analyzed to determine the fracture energy and peak load as indicators of adhesion strength between the sealant and the substrate.

As shown in Figures 11a and 11b, there were significant changes in both energy and peak load after paraffin wax was added to the asphalt binder. The fracture energy (Figure 11a) was increased after 1% of wax was mixed with the bitumen. However, there was a reduction of the fracture energy after 3% and 5% wax were added to the asphalt. This could be due to the presence of “bee” structures located in the asphalt that crystallize at low temperature (-12°C). Adding a small percentage of paraffin wax (1%) strengthens the bitumen bonding, as very little bee wax crystallizes at low temperature. An increase in wax leads to an increase in “bee” presence on the bitumen surface, which at lower temperature testing will crystallize and become brittle, requiring little energy to cause an adhesion failure. The same observation was done with the maximum load after the introduction of the wax. There was also an increase of the maximum load after adding 1% wax to the bitumen, but the maximum load was reduced after the wax was

increased to 3% and 5% (Figure 11b). This could also be due to the presence of bees that increase over the surface area of the bitumen as more and more paraffin is added. At a high percentage, the crystallized wax at low temperature will fail in adhesion after a small load is applied.

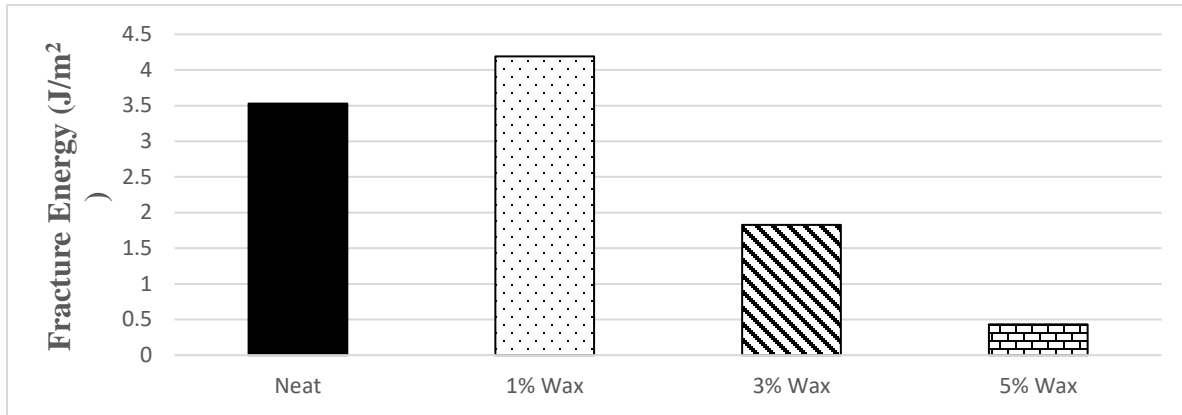


Figure 11a. DAT Fracture Energy Results for 0%, 1%, 3%, and 5% Wax-Modified Binder

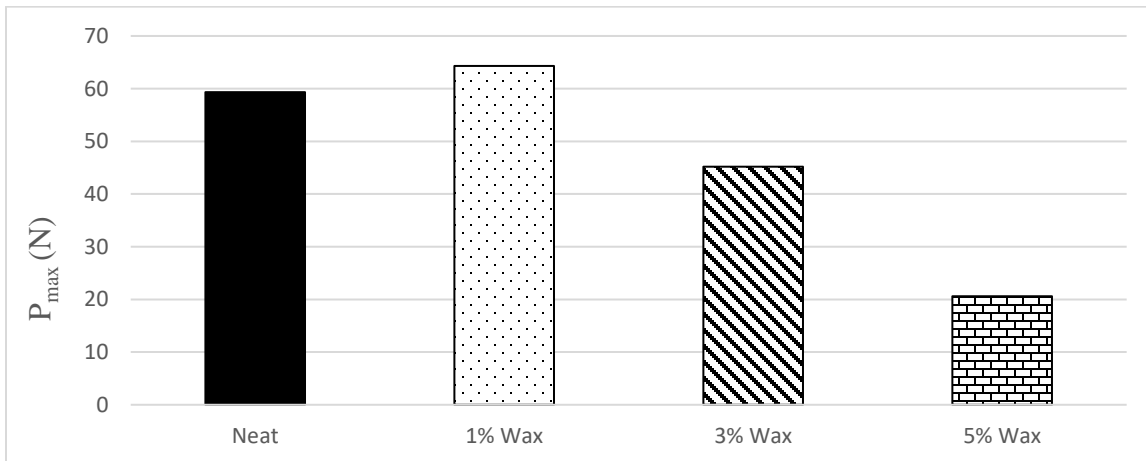


Figure 11b. DAT Peak Load Results for 0%, 1%, 3%, and 5% Wax-Modified Binder

#### 4.5 Fourier Transform Infrared Spectroscopy Analysis

The aging process of the joint sealant was further investigated using Fourier Transform Infrared Spectroscopy (FTIR) on the DD, EE, and FF crack sealants. FTIR is used to identify chemical functional groups by sending an infrared beam containing many different wavelengths through a sample to measure what wavelengths the medium absorbs (Bowers, 2013). Lu and

Isacson documented an increase in the carbonyl band (C=O) at approximately  $1700\text{ cm}^{-1}$  (Bowers, 2013). An increase in the carbonyl is a characteristic of an increase in the oxidation or aging of the asphalt binder; the same concept was applied for the DD, EE, and FF crack sealants with the area of focus for the carbonyl (C=O) at  $1700\text{ cm}^{-1}$  and saturated C-C stretch at  $2900\text{ cm}^{-1}$  for aging. The “peak area” method was also used to analyze the aging process.

Figures 12a, 12b, and 12c show the carbonyl formation and the saturated C-C band area for the field-aged FF, DD, and EE, and crack sealant. An increase of the peak area for the field-aged crack sealant at the  $1700\text{ cm}^{-1}$  wavenumber is noticeable. This is due to the stretch absorption of the carbonyl group. The reaction is due to a long-term exposure of the crack sealant in water, in this case rain, where the oxygen  $\text{O}_2$  from the  $\text{H}_2\text{O}$  element bonds with the carbon C located in the crack sealant, causing oxidation as aging occurs. Other factors involved in the aging process, such as sulphoxide bonding, are also involved in the aging process.

Additional FTIR analysis was conducted by investigating other crack sealants’ chemical properties after water exposure. All the sealants were exposed to water for 2, 4, and 8 weeks. Figures 12d - 12f show the FTIR results for virgin, lab-aged, and field-aged crack sealant after water exposure. As can be observed, the carbonyl formation seems to increase along with the water exposure time. The DD crack sealant for virgin, lab-aged and field-aged shows the highest carbonyl formation (94%, 97%, and 83%, respectively) after being exposed in water for up to 8 weeks. This indicates that the DD crack sealant ages more quickly than other crack sealants when exposed to water. Furthermore, the FF and EE crack sealants also show high carbonyl formation for the lab-aged and field-aged (100% and 56%, respectively), indicating that aging also occurs at a fast rate compared to other sealants. However, the BB and FF virgin sealants

showed the lowest increase of carbonyl overall (50% for both) after 8 weeks of water exposure. That implies that water causes aging of those sealants at a lower rate.

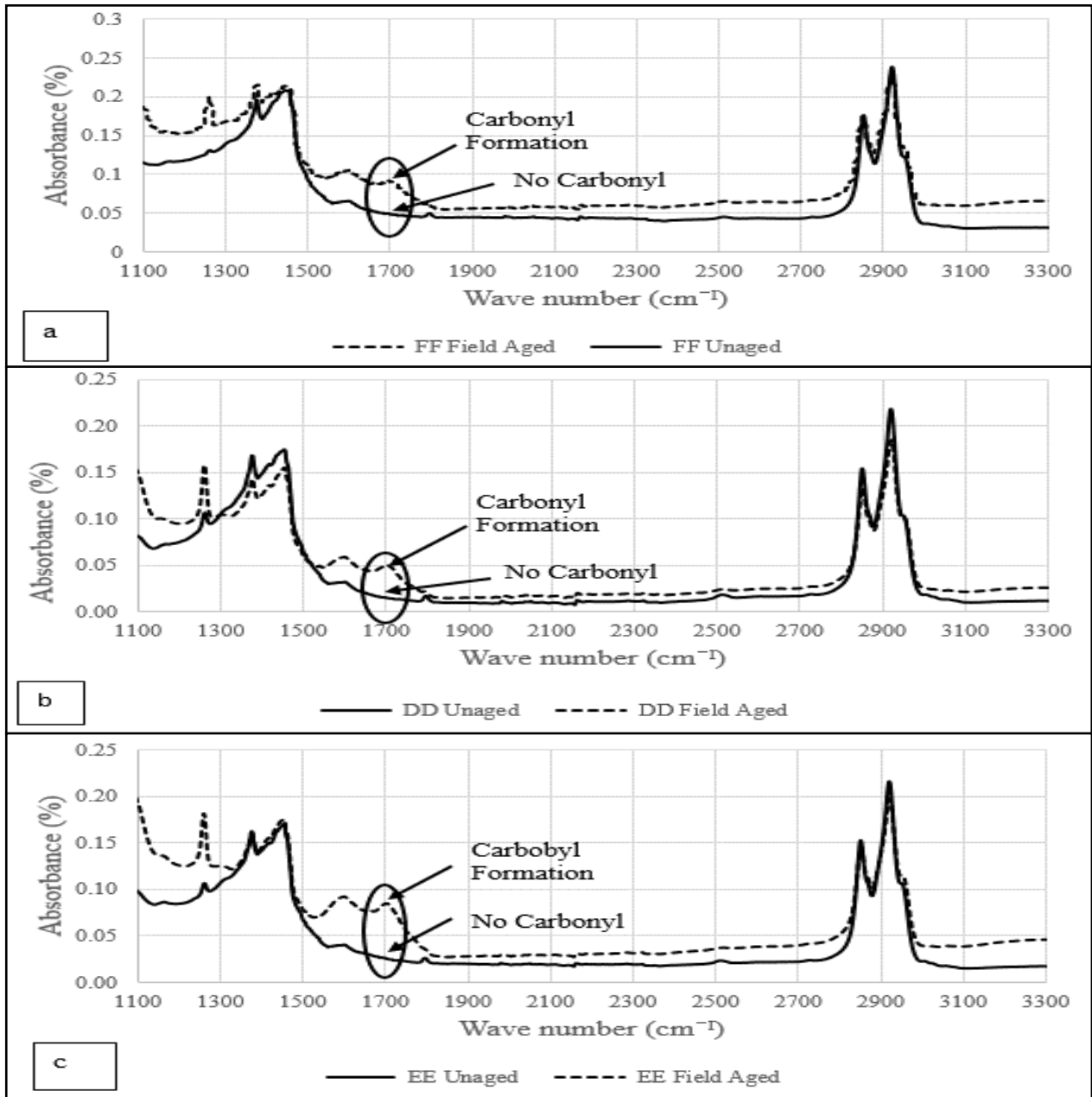


Figure 12a,b,c. Fourier Transform Infrared Spectroscopy Before and After Water Exposure

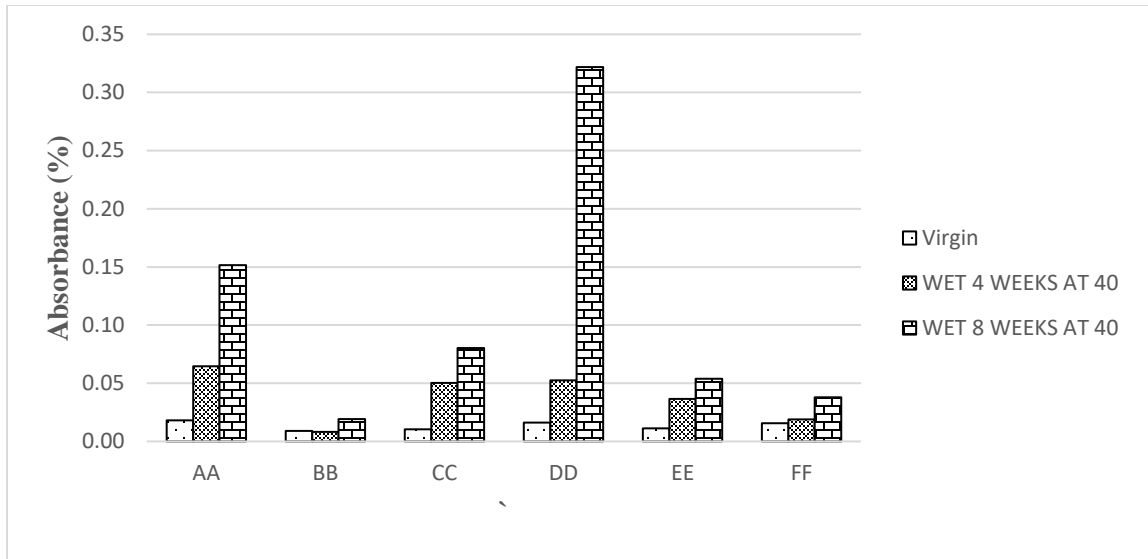


Figure 12d. Virgin Fourier Transform Infrared Spectroscopy Before and After Water Exposure

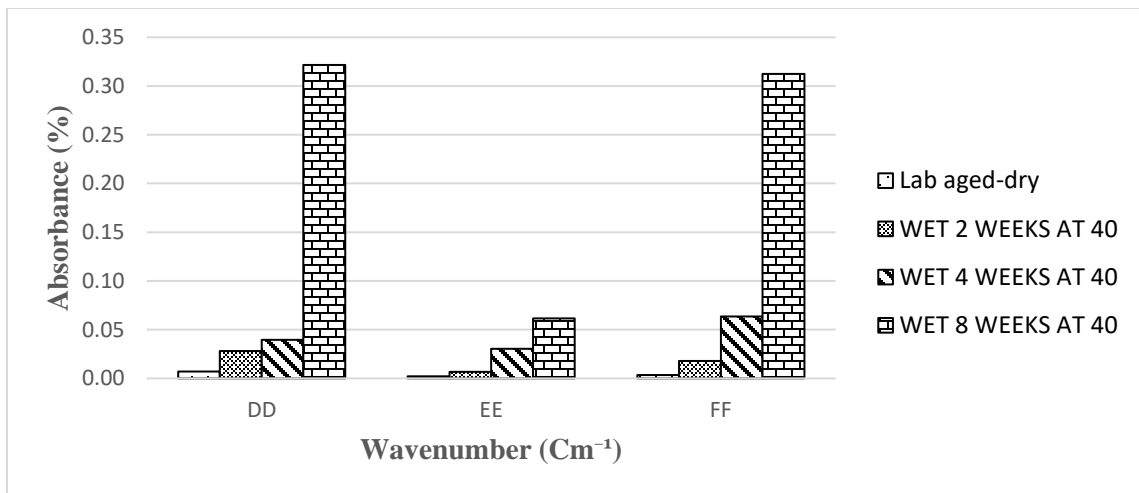


Figure 12e. Lab-Aged FTIR Before and After Water Exposure



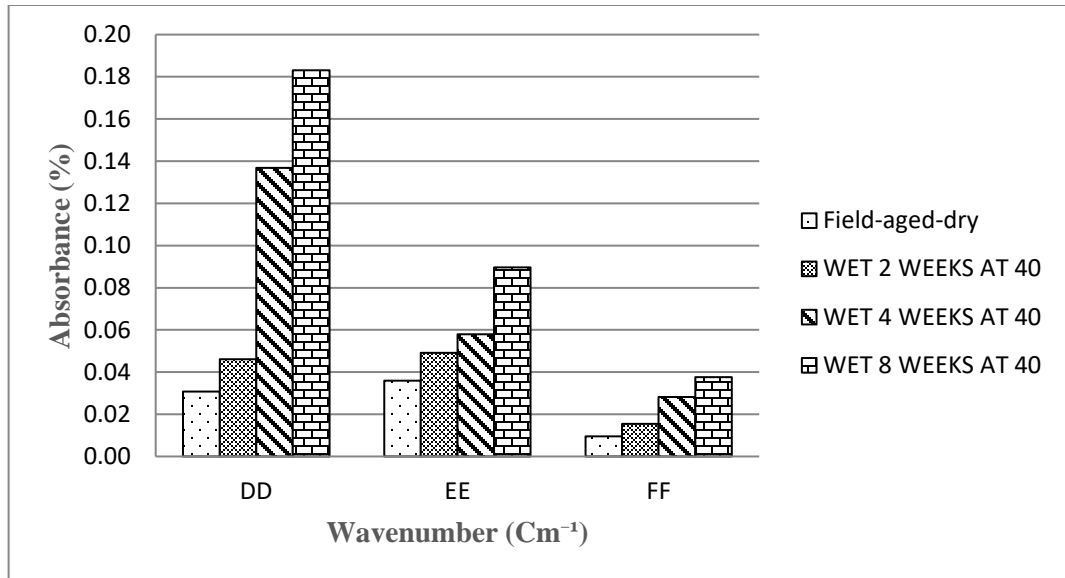


Figure 12f. Field-Aged FTIR before and after Water Exposure

#### 4.6 Sessile Drop Test

To further study the effect of water on the surface properties of sealant, contact angles between a droplet of water and the surface of each sealant were measured using a sessile drop method. The contact angle was used as a measure of sealant water phobicity and its surface interaction with water molecules. Furthermore, the effect of temperature on the contact angle was studied by conducting the experiment at temperatures ranging from 40°C to 80°C, representing pavement surface temperatures in a hot summer season. The latter test was conducted with the aid of an environmental chamber capable of sealing both pendent drop and the substrate surface, equipped with a temperature-control system synchronized with the test equipment (Figure 2).

It was observed that as the temperature increases, so does the contact angle (Figure 13a). However, the change in the contact angle varied among sealants, with the AA crack sealant being the least affected by the temperature. This was when water made the smallest contact angle with the AA crack sealant, indicating this sealant may have a good wettability with water. This

was when both BB and CC not only showed large contact angles, but also a large temperature dependence, showing a significant change in their contact angles with the increase in temperature. The observed variation of the contact angle could be attributed to changes in surface properties.

Furthermore, to study the interaction of a water droplet with conditioned sealants, contact angles between water-conditioned sealants and water were measured using a sessile drop method. To condition the sealants, each specimen was poured into an aluminum mold and was placed into water at 85°C for one hour. The aluminum mold was completely submerged in water, and the temperature was kept constant. Analysis of the contact angle results showed that the sealant contact angle varied significantly after conditioning (Figure 13b). Sealant CC showed a decrease in contact angle after conditioning, and its contact angle decreased as the temperature increased. However, both AA and BB crack sealants showed an increase in their contact angle after water conditioning, indicating a significant change in their surface properties after water conditioning.

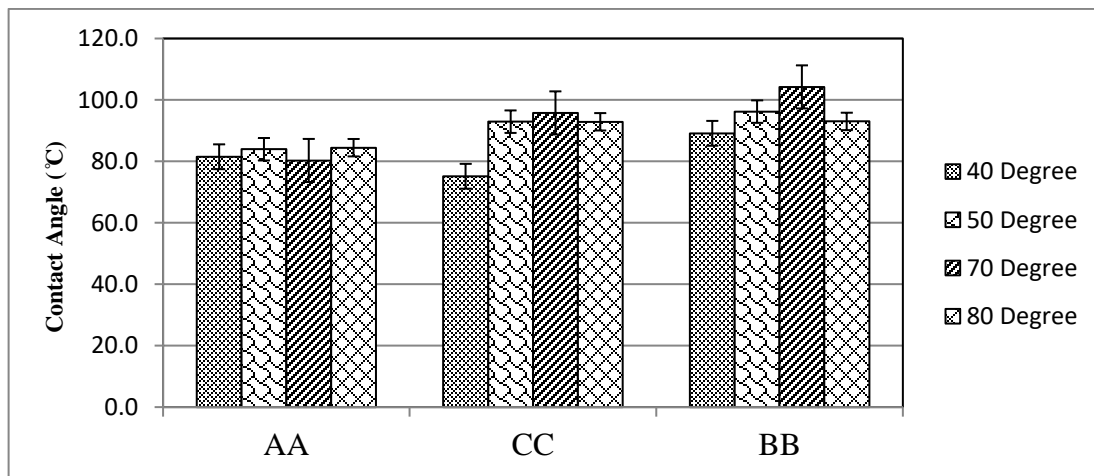


Figure 13a. Contact Angle Between Water and Dry Sealant at Various Surface Temperatures

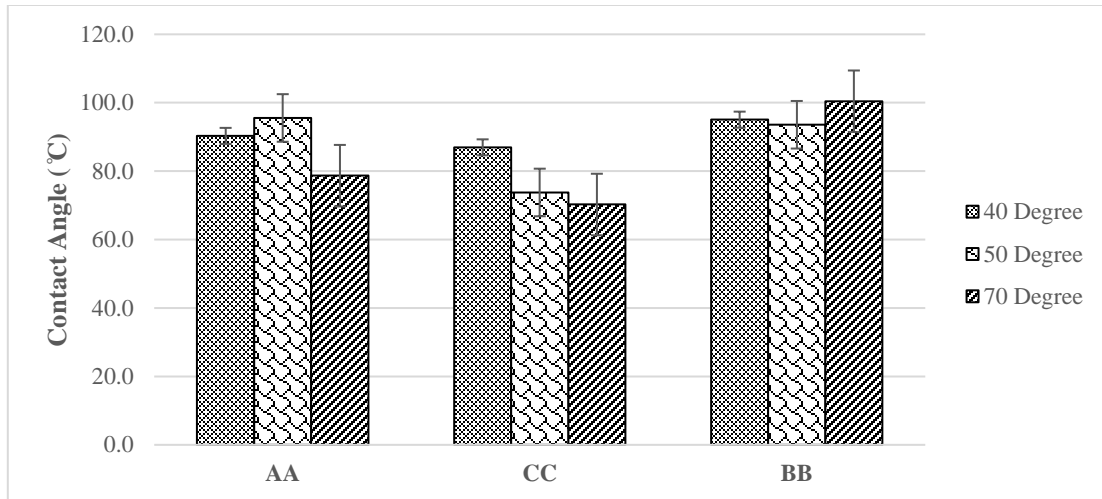


Figure 13b. Contact Angle between Water and Water-Conditioned Sealant at Various Surface Temperatures

#### 4.7 Crack Sealant Performance

To easily represent the water damage effect, a ranking was performed based on the change in peak area, the recovery and change in relaxation time between wet and dry crack sealant; using the direct adhesion test, the bending beam rheometer test, and the dynamic shear rheometer test result respectively. From table 4, the DAT shows that sealant DD has better adhesion than other crack sealants. This could refer to a much higher bonding with aggregate. Sealant FF has the worst property, and it is more susceptible to water damage than other crack sealants. The same observation was done using the BBR machine where the DD had the best performance with FF having the worst performance therefore it is most likely to fail. However, a different observation was done using the DSR. The FF crack sealant shows better recovery comparing to other crack sealants, followed by the EE crack sealant. This suggests that the stress dissipates faster than other crack sealants as the load applied are removed. The BB and DD crack sealants also show better stress dissipation after condition. The AA and CC crack sealant, however, has the worst property, and did not recover as other ones after conditioning.

Table 4. Overall Sealant Performance Based on Water Exposure Test

Ranking	DAT	BBR	DSR
1	DD	DD	FF
2	EE	CC	EE
3	BB	EE	BB
4	AA	BB	DD
5	CC	AA	AA
6	FF	FF	CC

#### 4.8 Asphalt Performance

The performance of the wax at different percentage on the asphalt viscosity was investigated. Figure 14a shows the viscosity measurement at 0%, 1 %, 3% and 5% wax at different temperature under 50 rotations per minute (rpm). The graph shows a significant difference of viscosity between the 0% wax and the 5% wax at 105°C. The viscosity drops as more wax is added. Also, an increase in temperature reveals lower viscosity which decreases as the temperature is augmented to 150°C. This is due to the amount of “bee” wax that dissolves at higher temperature. Adding wax increases the presence of “bee” wax in the asphalt binder. At low temperature such as 105°C, only few “bees” are affected at that temperature increasing the viscosity. Upon increasing the temperature up to 150°C, those “bees” wax dissolve reducing the viscosity of the asphalt binder.

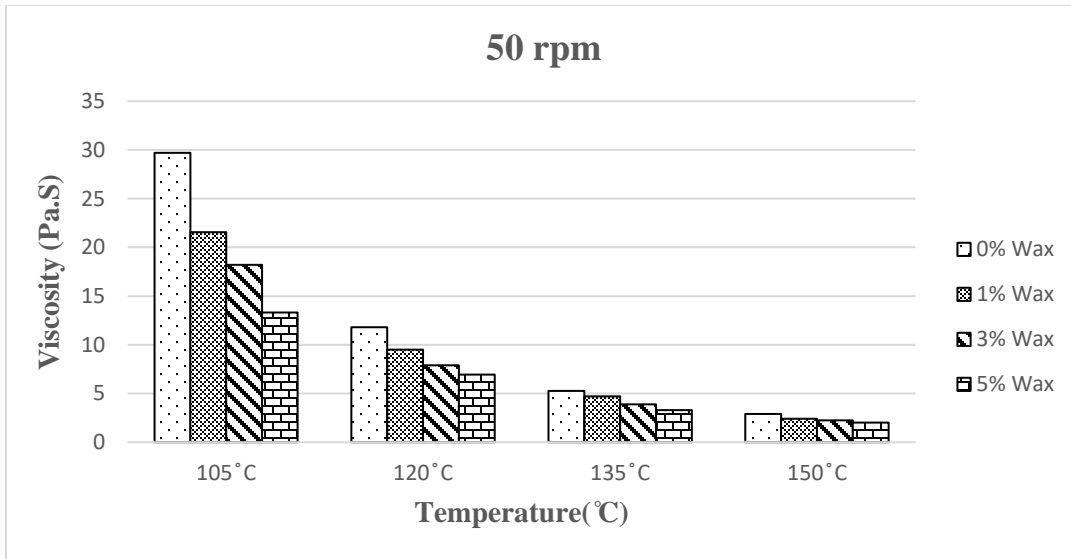


Figure 14a. Viscosity vs Temperature at 0%, 1%, 3%, and 5% wax under 50 rpm.

Figure 14b shows the viscosity measurement for the 0%, 1 %, 3% and 5% wax at 20 and 50 rpm. Measurements were done at 135°C. The result reveals a significant decrease in viscosity for the neat binder (0% wax) between 20 and 50 rpm. The viscosity appears to be very high at low concentration wax doped and decreases as the wax percentage and speed increase. This could be due to the amount of wax absorbed during a rotational speed within a specified time. So a 1% dosage will release wax that will be absorbed during a rotational speed causing higher viscosity than a 3% wax. At 5% concentration, the wax content increases but less wax is absorbed due to the saturation of the binder causing low viscosity at higher speed.

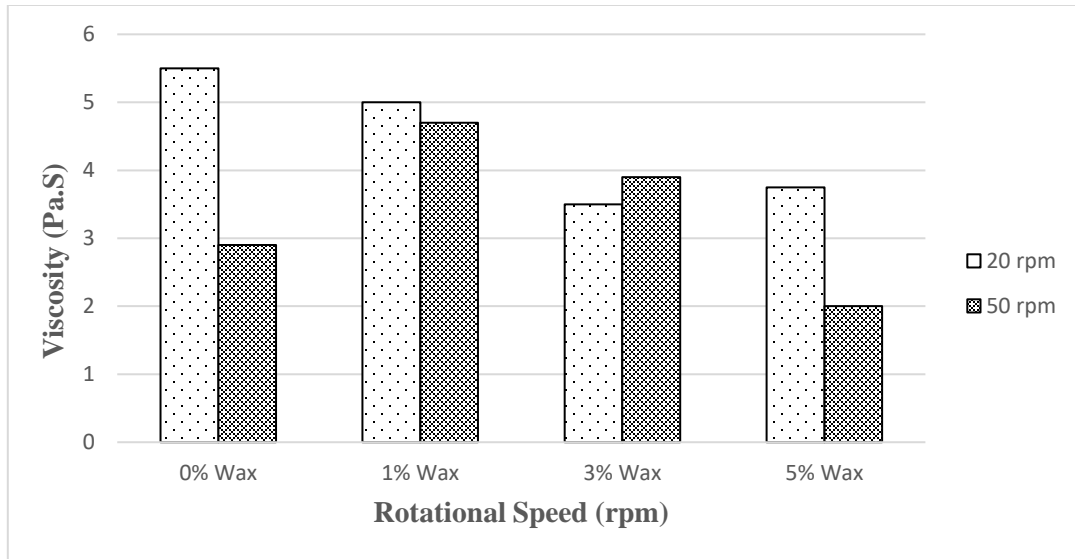


Figure 14b. Effect of Rotational Speed on Asphalt Binder at 0%, 1%, 3%, and 5% Wax Under 20 rpm and 50 rpm

#### 4.8.1 Temperature susceptibility

The measurement of asphalt binder viscosity was done under various temperatures. The following equation (eq. 1) has been commonly used to calculate the viscosity-temperature susceptibility (VTS) (Rasmussen et al., 2002).

$$VTS = \frac{[\log(\eta_{T_2}) - \log[\log(\log(\eta_{T_1}))]]}{\log(T_2) - \log(T_1)} \quad \text{Equation (1)}$$

T1 and T2 are the temperatures of the binder at known points;  $\eta_{T_1}$  and  $\eta_{T_2}$  are the viscosities of the binder at the same known points (cP).

The temperature susceptibility was further investigated by calculating the VTS value using Equation 1. It is desired for the asphalt binder to have lower temperature susceptibility. Figure 15 shows a very high VTS graph that decreases as the wax percentage is increased. The 5% wax shows the lowest VTS value, indicating a reduction of the temperature susceptibility of the asphalt binder. This reduction is due to the presence of the wax in the asphalt matrix.

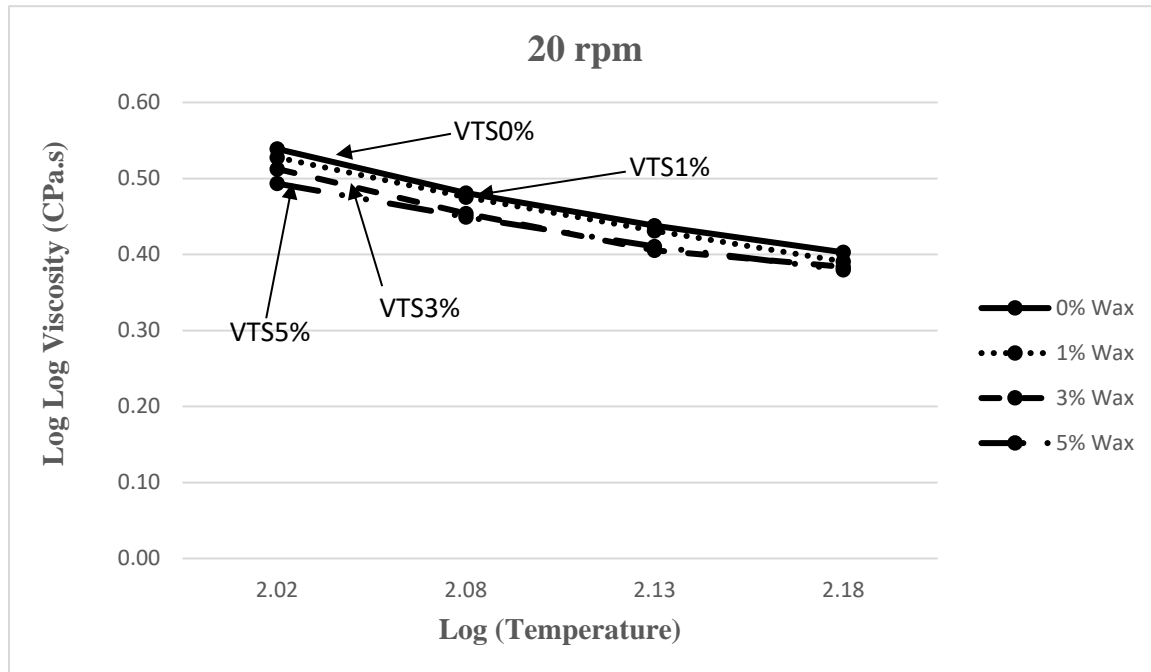


Figure 15. Viscosity vs. Temperature for 0%, 1%, 3%, and 5% Wax at 20 rpm

#### 4.8.2 Shear susceptibility

The rate of change in viscosity with the shear rate is called shear susceptibility. The shear susceptibility (also known as the shear index) is determined by calculating the slope of the line formed by a log of rotational speed versus the log viscosity graph using Equation (2) (Roberts et al., 1996).

$$SS = \frac{\log(\text{viscosity})}{\log(\text{speed})} \quad \text{Equation (2)}$$

Asphalt binder with lower shear susceptibility typically shows better performance (Roberts et al., 1996). The investigation of shear susceptibility was done using Equation 2, then was plotted at different times. Figure 16 shows that as the wax percentage increases, the shear rate susceptibility decreases. Raising the wax percentage leads to the release of “bee” wax in the

asphalt binder, causing uniform concentration and making the asphalt binder less susceptible to shear rate.

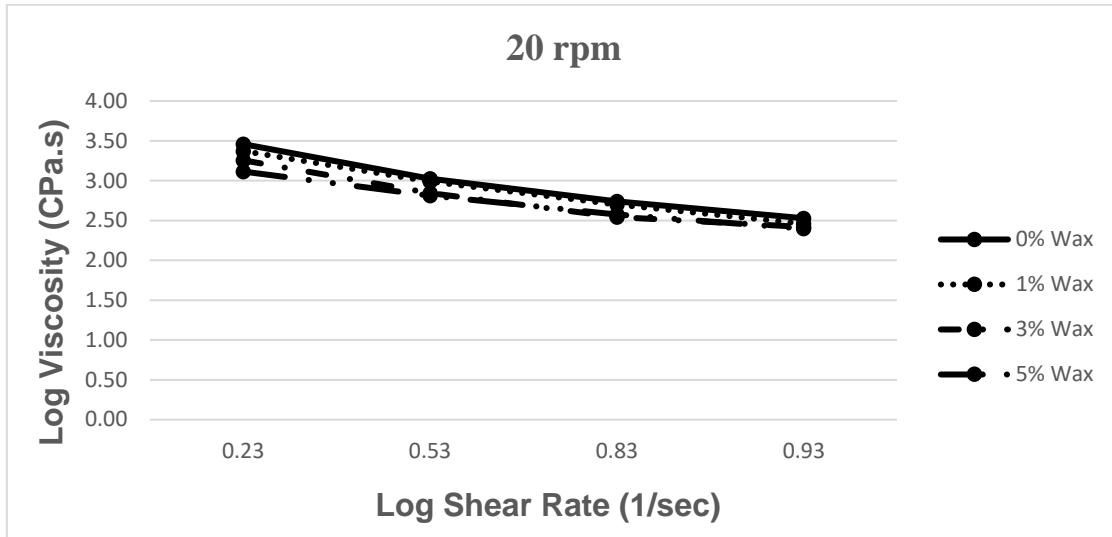


Figure 16. Shear Susceptibility of 0%, 1%, 3%, and 5% Wax at 20 rpm

#### 4.9 Direct Tension Test

Figure 17a shows the fracture energy from the direct tension test (DTT). This relates to the binder’s cohesive properties, as the amount of energy required to break or fracture the sample is determined. The results show that with 1% wax modification, the fracture energy was significantly reduced. This is consistent with the corresponding crossover temperature and the DAT results. A slight reduction was also observed at 5% wax; though it is within the standard error of 3% wax, it does not follow the expected trend of consistent significant increase. Since fracture energy is a result of both peak load and ductility results, it is important to analyze both measured properties to better understand the fracture energy results in Figure 17a.

Figure 17b shows that both the peak load and ductility are significantly lower for the binder with 1% wax than for the neat binder. This means that the low fracture energy results observed in Figure 17a are not simply a result of ductile failure and do not need to be tested at a



lower testing temperature. Though the ductility appears to increase significantly at 3% wax, the ductility results for 3%, 5%, and 10% wax are still significantly lower than for the neat binder. The loss in ductility attests to the binder's decreased ability to stretch, which is also reflected in the significant increase in peak loads for the corresponding samples. This is consistent with the behavior observed from the BBR and DAT results.

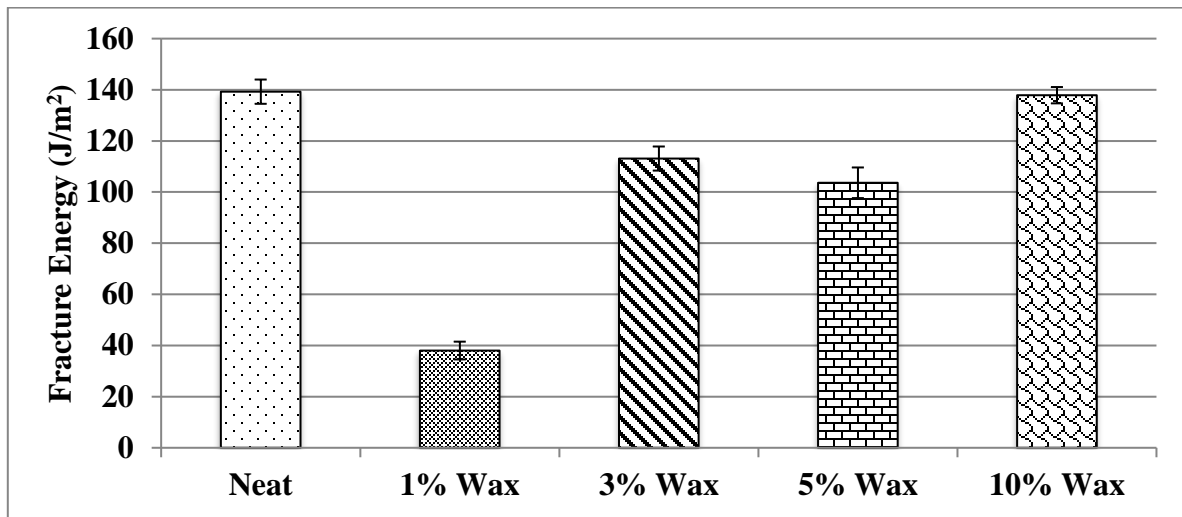


Figure 17a. DTT Fracture Energy for 0%, 1%, 3%, and 5% Wax-Modified Binder

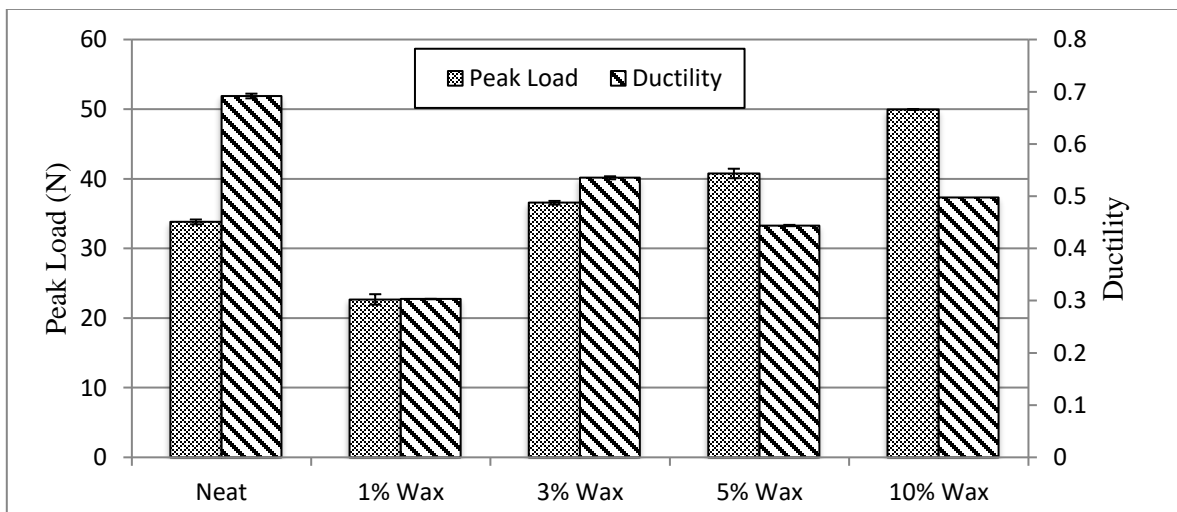


Figure 17b. DTT Peak Load and Ductility for 0%, 1%, 3%, and 5% Wax-Modified Binder

#### 4.10 Differential Scanning Calorimetry

Figures 18a and 18b show the glass transition temperature and the heat capacity of the wax-modified bitumen samples, using the modulated differential scanning calorimetry (MDSC) method. As can be seen, the glass transition phase heat capacity increases with an increase of wax content. On the other hand, the total energy to heat the sample with 5% added wax is higher than the other samples. Another observation is that the heat capacity of 10% binder is lower than for 3% and 5%, after the glass transition phase.

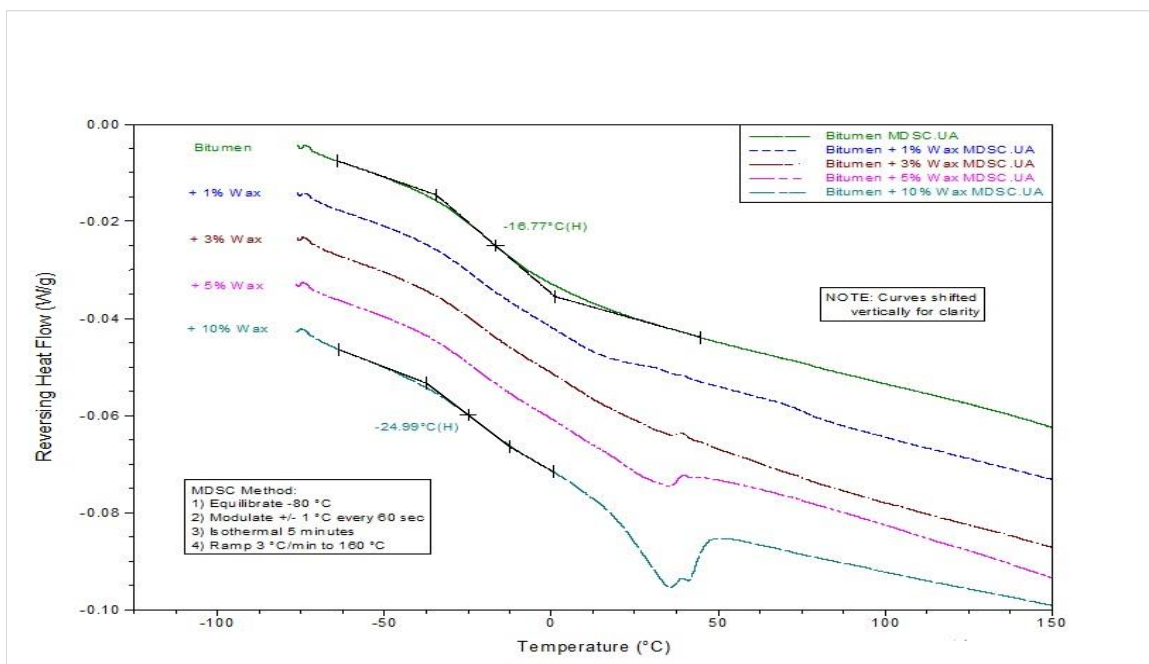


Figure 18a. Glass Transition Temperature (T<sub>g</sub>) for Different Wax-Modified Bitumen, Using the MDSC method

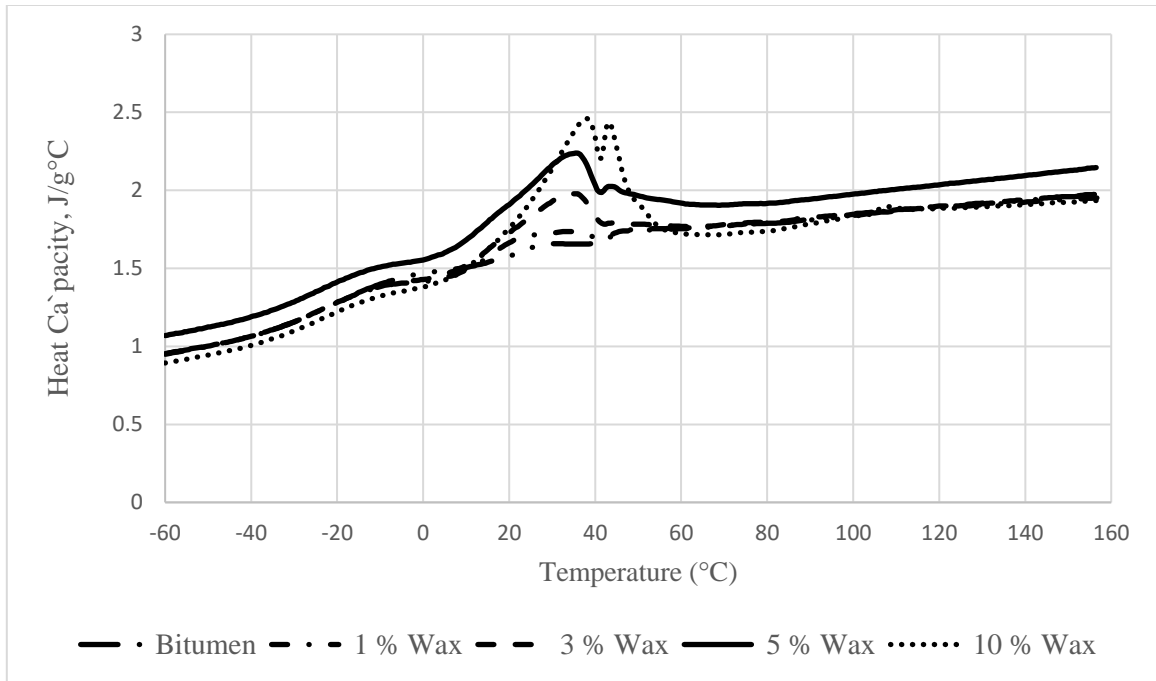


Figure 18b. Comparison of Heat Capacity of Samples With Different Amounts of Added Wax

#### 4.11 Atomic Force Microscopy

To further examine the effect of wax on bee formation, a study of the surface morphology of asphalt doped with various percentages of wax (0%, 1%, 3%, and 10%) was conducted. Atomic force microscopy (AFM) images of freeze-fractured bitumen surfaces were previously reported exhibiting circular features roughly 10 – 20  $\mu\text{m}$  in diameter (Fischer and Dillingh, 2015). However, moisture from the air could have condensed on the cold fractured surface, and water is known to alter the surface texture of bitumen (Santos et al., 2014). Experiments showed that 10 – 40  $\mu\text{m}$  droplets of water condensed on a bitumen surface stored under 100 % humidity at room temperature can significantly distort the morphology of an asphalt surface (Hung et al., 2015).

Figure 19a shows AFM images of the native air surface and the bulk fracture surface of undoped, 1% wax-doped, and 3% wax-doped bitumen. The bee structures at the air surface grow in size, amplitude, and wavelength with increasing wax content, consistent with previous studies.

Figure 19b shows that with 10% added wax, the bee structures on the surface disappear and are replaced by a lamellar, terraced topography common to paraffin wax. The thickness of the lamellae here is 3 – 5 nm. The difference may be due to either a difference between lateral resolutions versus depth resolution in AFM or a difference between the thicknesses of lamellar wax crystals in the bulk compared to surface.

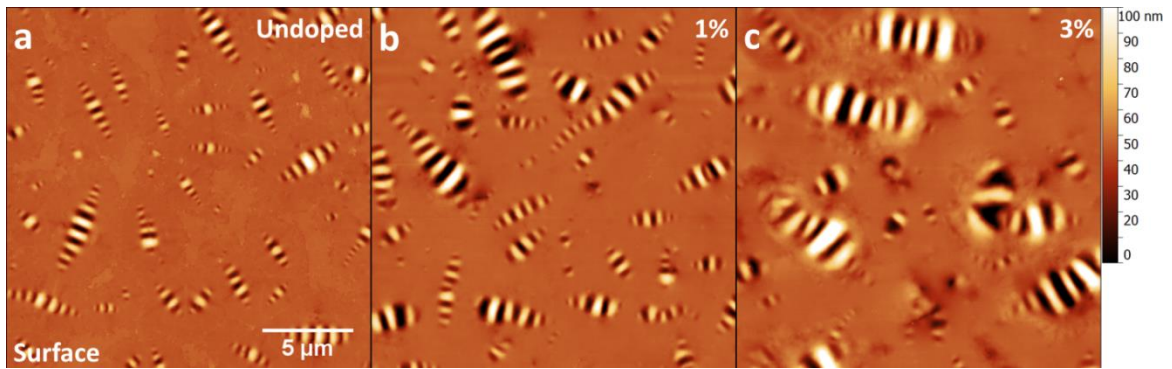


Figure 19a. AFM Images of the Surface of Bitumen Samples Doped With Paraffin Wax (0%, 1%, and 3%, by Weight of Base Asphalt)

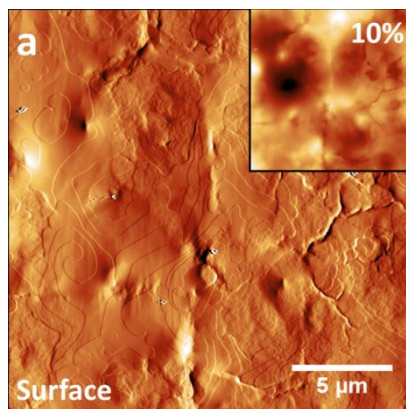


Figure 19b. AFM Amplitude Image of the Surface of 10% Wax-Doped Bitumen

## Chapter 5

### Conclusions

#### 5.1 Crack Sealant

Crack sealants are used to prevent water from entering between the joints. However, extended exposure to water causes the crack sealant to fail. Using the appropriate sealant for different climates and conditions is very important. This study examines the effect of water on the rheological and chemical properties of crack sealant.

The DSR test shows the relaxation time before and after conditioning. The relaxation time increases for wet sealant and the modulus also increases for the most part. The DSR ranking shows that the FF sealant is better than the CC sealant after conditioning.

The Extended BBR test was performed to measure low-temperature susceptibility. The DD crack sealant appears to be faster to recover at low temperature. The FF crack sealant, however, was the slowest, disagreeing with the DSR result.

The DAT conducted was to determine the sealant with better resistance to failure after conditioning. The result shows the DD crack sealant is the best to resist adhesion failure. The FF crack sealant was the lowest and easiest crack sealant to fail when different loads were applied.

FTIR was used to find the aging that occurs at the molecular level. The result shows that oxidation is the main reason why materials age. The oxygen from water bonds with the carbon in the sealant to enable oxidation. The presence of carbonyl determines the aging of the sealant. The EE crack sealant showed the highest aging, followed by the DD and FF crack sealants after two years of exposure. The test overall shows that the DD crack sealant has the best water resistant property; the FF crack sealant has the worst property and is more susceptible to fail after water exposure.

The contact angle between a droplet of water and a sealant surface was measured at different temperatures. The study results showed that B-195 crack sealant has the highest contact and the highest sensitivity to temperature variation. This was also in agreement with the direct adhesion test results indicating the highest drop in energy and peak load as a result of water conditioning. This in turn indicates that B-195 is most susceptible to water; this was followed by sealant type 4, while sealant type I was found to be the least susceptible to water.

## **5.2 Asphalt**

The RV result shows that at high temperature, the viscosity decreases as more wax is added to the asphalt binder. A decrease in viscosity and a reduction in shear susceptibility are also observed once the wax percentage is increased.

From the intermediate temperature results from the DSR, increasing the wax percentage leads to a decrease in complex modulus at high-intermediate temperatures and an increase in modulus at low-intermediate temperatures, which is consistent with previous research using wax. However, when observing the crossover temperature, 1% wax was actually lower than the neat binder.

The experiment analysis performed using atomic force microscopy (AFM) on a wax-doped asphalt complex further showed the appearance of coarser surfaces as the percentages of wax increased from 1% to 3%. A fractured surface in non-wax bitumen was found to be quite smooth. However, the fracture surfaces continued to become rougher as the wax content increased ( $R_q = 4.1 \text{ nm}$  at 3 % wax, and  $R_q = 340 \text{ nm}$  at 10% wax). Analysis of AFM images further showed as the wax content increases, so does the bee wavelength.

The DSC result shows that adding wax to neat binder lowers the glass transition temperature, which can result in higher resistance to low-temperature cracking. Bitumen binder

with higher wax content has lower energy consumption needed to attain the mixing and compaction temperature.

Extended BBR results show that increasing the wax percentage leads to a stiffer binder with a decreased ability for stress relaxation (m-value).

DAT results show that an increase in wax percentage leads to an initial increase in fracture energy at 1%, then a decrease in energy after progressively more wax is added. The same observation was done with the fracture load, which also increases at 1% wax before decreasing when higher wax dosages are added. However, the change in fracture energy is higher as the wax is increased, compared to the change in fracture load.

DTT results show that increasing the wax percentage initially leads to a significant drop in fracture energy at 1% wax; the fracture energy then shows a general trend of increase similar to that of the neat binder. However, after investigating the peak loads and ductility results, it was shown that the increase in fracture energy is a result of increasing peak load and slightly decreasing ductility, which reflects the increasing dominance of the paraffin wax crystal structure within the binder.

## References

1. White, C.C.; Tan, K.T.; O'Brien, E.P.; Hunston D.L.; Chin, J.W.; Williams, R.S. (2011). Design, Fabrication, and Implementation of Thermally Driven Outdoor Testing Devices for Building Sealants. National Institute of Standards and Technology: 1-9.
2. Al-Qadi, I., Yang, Sh., Fini, E., Masson, J-F., and McGhee, K. (2009). Performance-Based Specification for the Selection of Bituminous-Based Hot-Poured Crack Sealants. Journal of the Association of Asphalt Paving Technologists. 491-533
3. Edwards, Y., and Redelius, P. (2003). "Rheological Effects of Waxes in Bitumen." American Chemical Society Journal, 17: 511-520.
4. Paving, A. (2016, May 04). Alpha Paving Industries. Retrieved from Alpha Paving Texas: <http://www.alphapavingtexas.com/faq-answer/difference-hot-pour-cold-pour-crack-sealants/>
5. Yetkin, Y., Qatan, A., & Kennedy, T. (2003). Performance evaluation of hot and cold pour crack sealing treatments on asphalt surfaced pavements. *Performing Organization Report*. 1-84
6. Masson, J-F., Collins, P., Legare, P-P. (1999). Performance of pavement crack sealants in cold urban conditions. *Institute for Research in Construction*. 26:395-401.
7. Yetkin, Y., Qatan, A., & Kennedy, T. (2002). Performance Evaluation of Hot and Cold Crack Sealants Treatments on Asphalt Surfaced Pavements. *Performing Organization Report*. 1-84
8. Dos Santos S., M. N. (2015). "From virgin to recycled bitumen: A microstructural view." ScienceDirect, 177-185.
9. Masson, J-F.; Lauzier, C.; Collins, P.; Lacasse, M.A. (1998) "Sealant Degradation During Crack Sealing of Pavements." Journal Of Materials in Civil Engineering. 250-255.
10. Fischer H. R., Dillingham E. C., Hermse C.G.M., (2013). "On the microstructure of bituminous binders." Road Materials and Pavement Design, 1-16.
11. White, C. C.; Tan, K. T.; Hunston, D. L.; Williams, R. S.. (2009). Durability of building joint sealants. Service Life Prediction of Polymeric Materials 115-128.
12. Fang, C., Galal, K., Ward, D., Haddock, J. (2003). Cost-Effectiveness of Joint and Crack Sealing. Performing Organization Report. 1-258.
13. Lacasse, M.A, and Masson, J-F. (2004). Developing a Performance-Based Joint Sealant Specification for Airport PCC Pavements. Institute for Research in Construction. 1(7):1-9.
14. Masson J-F. (2014). Bituminous Sealants for Pavement Joints and Cracks: Building the Basis for a Performance-Based Specification. Institute for Research in Construction. 1-13
15. Ashok, G., Tianxi, T., & Dan, Z. (1997). Evaluation of Joint Sealants of Concrete Pavements. Performing Organization Report. 1-149.
16. Al-Qadi, I., Yang, W., Fini, E., Masson, J.-F. (2008). Towards performance-based selection guidelines for roadway crack sealants. Institute for Research in Construction. 1-12
17. Goodwin, A.; Hung, A.; & Fini, E. (2015). "Effects of water on bitumen surface microstructures at elevated temperature or increased exposure time." 1-9.



18. Fini, E, I. Al-Qadi, T. Abu-Lebdeh, and Masson, J-F.. (2011). Use of Surface Energy to Evaluate Adhesion of Bituminous Crack Sealants to Aggregates. *American Journal of Engineering and Applied Sciences*. 244-251
19. Al-Qadi, I, and Fini, E.(2013). Development of a Crack Sealant Adhesion Test Specification for Hot-Poured Bituminous. *Journal of Testing and Evaluation*. 39(2): 1-7.
20. Fischer, H. R., & Dillingh, B. (2015). "Response of the microstructure of bitumen upon stress–damage initiation and recovery." *Road Materials and Pavement Design*, 16.1 (2014): 31–45. Print.
21. Allen, J. S. (2003). An Analytical Solution for Determination of Small Contact Angles from Sessile Drops of Arbitrary Size. *Journal of Colloid and Interface Science*. 481–489.
22. Pozrikidis, A. H. (2013). Deformation of an Elastic Substrate Due to a Sessile Drop. *European Journal of Mechanics*. 90–99.
23. Haithem, S., and Shalaby ,A.(2007). Evaluation of Joint and Crack Sealants Based on Cyclic Loading and Rheological Properties. *Transportation research Board*. 1-12.
24. Lu, X. and Redelius, P. (2006). "Effect of Bitumen Wax on Asphalt Mixture Performance." *ScienceDirect*, 21: 1961-1970.
25. De Moraes, M.B; Pereira, R.B.; Simao, R.A ; and Leite, L.F.M. (2009). "High Temperature AFM Study of CAP 30/45 Pen Grade Bitumen." *Journal of Microscopy*, Vol 239: 46–53.
26. Dos Santos S., M. N., Poulikakos L.D., (2014). “Newly observed effects of water on the microstructures of bitumen surface.” *Construction and Building Materials*, 618–627.
27. CrafcO. (2008,2010, January, March). Product Data Sheet. Retrieved July 30, 2014, from <http://www.crafcO.com>
28. Al-Qadi, I., Yang, Sh., Fini, E., Masson, J-F., and McGhee, K. (2009). Performance-Based Specification for the Selection of Bituminous-Based Hot-Poured Crack Sealants. *Journal of the Association of Asphalt Paving Technologists*. 491-533.
29. Marmur, A. Soft contact: measurement and. [www.rsc.org/softmatter](http://www.rsc.org/softmatter), pp.12-17 last accessed July 30, 2014.
30. Lee, Y. Y. (2013).Contact Angle and Wetting Properties. *Springer*.51:3-34.
31. Bowers, B. F. (2013). Investigation of Asphalt Pavement Mixture Blending Utilizing Analytical Chemistry Techniques. *Tennessee Research and Creative Exchange*.1-195.
32. Fischer, H. R. and Dillingh, B. (2015). *Road Materials and Pavement Design*. 16 p. 31-45.
33. Rasmussen, R.O., L. Robert L., and C. George K. (2002). “Method to Predict Temperature Susceptibility of an Asphalt Binder.” *Journal of Materials in Civil Engineering*. 14: p. 246-252.
34. Santos, S. D., Partly, M. N. and Poulikakos, L. D. (2014). *Construction and Building Materials*. 71 p. 618-627.
35. Roberts, F. L., P. S. Kandhal, E. R. Brown, D. Y. Lee, and T. W. Kennedy.Hot Mix Asphalt Materials, Mixture, Design, and Construction. *National Asphalt Pavement Association Research and Education Foundation,Lanham, Md., 1996*